



Contents lists available at ScienceDirect

Gondwana Research

journal homepage: [www.elsevier.com/locate/gr](http://www.elsevier.com/locate/gr)

# The petrogenesis of ultramafic rocks in the > 3.7 Ga Isua supracrustal belt, southern West Greenland: Geochemical evidence for two distinct magmatic cumulate trends

Kristoffer Szilas<sup>a,b,\*</sup>, Peter B. Kelemen<sup>a</sup>, Minik T. Rosing<sup>b</sup>

<sup>a</sup> Lamont-Doherty Earth Observatory of Columbia University, 61 Rt. 9 W, Palisades, NY 10964-8000, USA

<sup>b</sup> Natural History Museum of Denmark, Nordic Center for Earth Evolution, University of Copenhagen, Øster Voldgade 5-7, 1350 Copenhagen K, Denmark

## ARTICLE INFO

### Article history:

Received 2 May 2014

Received in revised form 7 July 2014

Accepted 10 July 2014

Available online xxxxx

Handling Editor: T. Kusky

### Keywords:

Serpentinite

Fractional crystallisation

Harzburgite cumulate

Platinum-group elements

## ABSTRACT

Ultramafic rocks with MgO > 25 wt.% are found as large slivers within the Eoarchean Isua supracrustal belt. Some of these ultramafic bodies have previously been proposed to represent relicts of residual mantle. In this study we present new bulk-rock major, trace and platinum-group element data, as well as mineral chemistry for these rocks in order to constrain their origin.

The ultramafic rocks form two distinct geochemical trends, which project away from local tholeiitic basalts and boninite-like volcanic rocks, respectively. The ultramafic rocks have FeO<sub>t</sub> contents of up to 16 wt.% and Al<sub>2</sub>O<sub>3</sub> up to 11 wt.%, with abundant normative orthopyroxene. Their trace element patterns are broadly parallel with the two types of volcanic rocks with which they are associated. All analysed rocks have fractionated chondrite-normalised platinum-group element patterns with relatively low Os and Ir abundances. The few spinel grains that were found to be potentially primary (Fe<sup>3+</sup># < 10) have Cr# of around 73 and most have Mg# of about 23. None of the above geochemical features are compatible with a residual mantle origin of the ultramafic rocks in the Isua supracrustal belt. Instead, these data suggest an origin of the ultramafic rocks by accumulation of mainly olivine + spinel during fractional crystallisation of the tholeiitic basalts and the boninite-like volcanic series, and possibly continued crystallisation of plagioclase ± orthopyroxene to form the more Al-rich cumulates. This interpretation is supported by modelling of the liquid evolution and the corresponding bulk-cumulates, for the two volcanic sequences. We find that the observed and calculated liquid evolutions match reasonably well, and can be explained mainly by olivine and spinel crystallisation. However, depending on the amount of accumulated plagioclase and orthopyroxene, the observed bulk-cumulate requires additional input from the evolving liquids to account for the elevated SiO<sub>2</sub>, Al<sub>2</sub>O<sub>3</sub>, TiO<sub>2</sub>, normative orthopyroxene and the trace element abundances of the ultramafic rocks.

We conclude that igneous crystal fractionation, in combination with cumulate–liquid interaction is capable of explaining all of the geochemical variation observed for these ultramafic rocks, and that there is no evidence for residual mantle rocks in the Isua supracrustal belt.

© 2014 International Association for Gondwana Research. Published by Elsevier B.V. All rights reserved.

## 1. Introduction

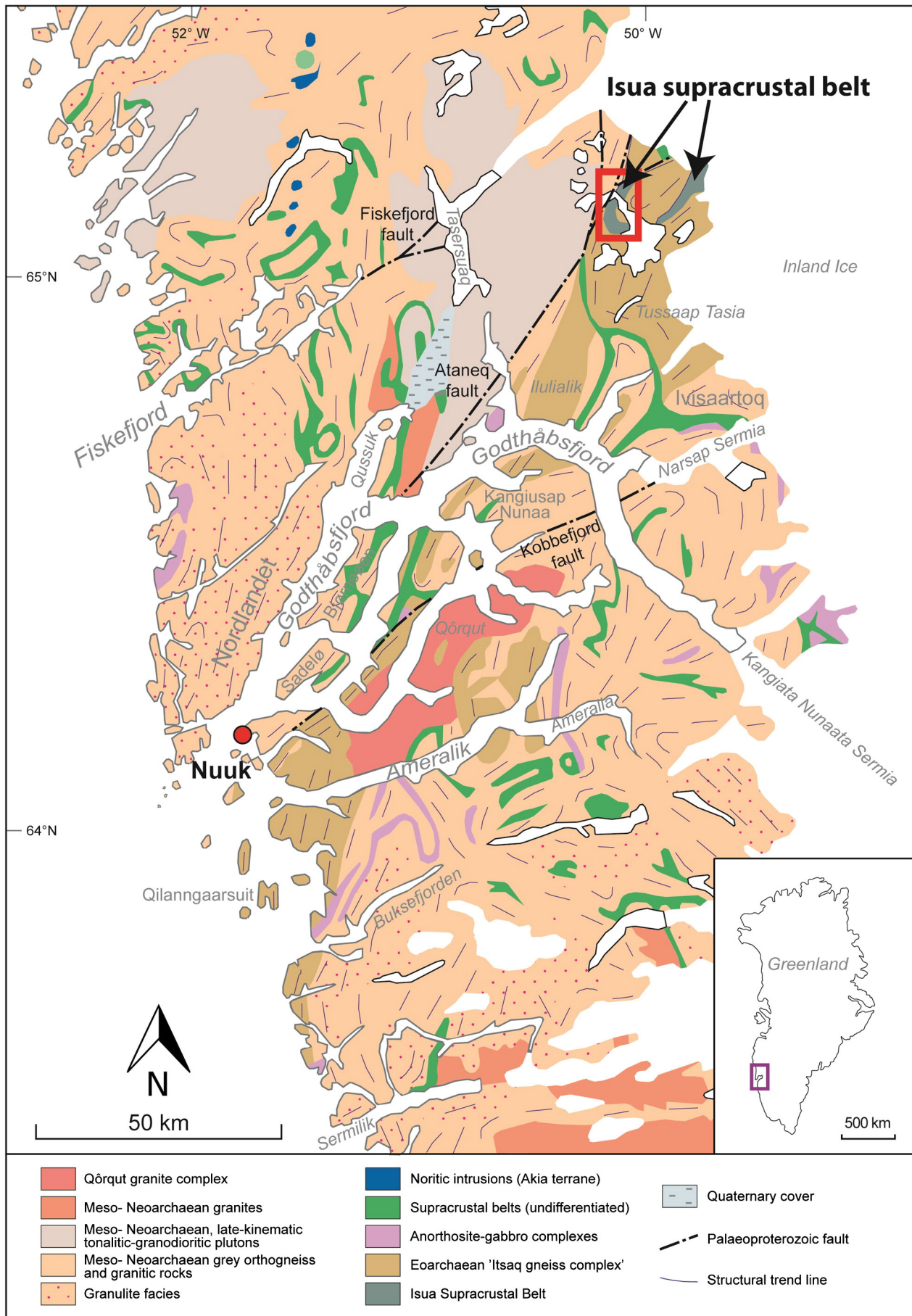
The Archaean supracrustal belts of southern West Greenland have many geochemical features which indicate formation in a subduction zone setting, and include rocks of boninitic and andesitic affinity and mafic intrusions with primary hydrous phases (e.g., Garde, 2007; Polat et al., 2008, 2012; Kisters et al., 2012; Szilas et al., 2012a,b, 2013a; Nutman et al., 2013; Huang et al., 2014). Even the Eoarchean Isua supracrustal belt (Fig. 1) is considered by most authors to be arc-related (Polat et al., 2002, 2003; Dilek and Polat, 2008; Appel et al., 2009; Furnes et al., 2009; Friend and Nutman, 2010; Polat et al., 2011). There is controversy surrounding the possibility of a sheeted

dike complex within the Isua supracrustal belt, and thus disagreement on whether or not this rock association represents an ophiolite sensu stricto (see Furnes et al., 2007a,b; Hamilton, 2007; Nutman and Friend, 2007a). Another standing question is the potential for the occurrence of depleted dunitic mantle residues within the Isua supracrustal belt, as proposed by Friend and Nutman (2011). Regardless of the geodynamic origin of such mantle rocks, these would obviously be a unique source of direct information about Earth's mantle evolution through time. However, given the implications of this interpretation, the hypothesis that ultramafic rocks of the Isua supracrustal belt represent mantle residues needs to be rigorously evaluated.

In the present study, we provide new constraints for the origin of these ultramafic rocks in the form of a geochemical data set for 52 samples from the western arm of the Isua supracrustal belt (Fig. 2). Several alternative origins can be imagined for these ultramafic rocks, including: (1) ultramafic magmas (komatiites), (2) ultramafic cumulates, or

\* Corresponding author at: Lamont-Doherty Earth Observatory of Columbia University, 61 Rt. 9 W, Palisades, NY 10964-8000, USA.

E-mail address: [kszilas@ldeo.columbia.edu](mailto:kszilas@ldeo.columbia.edu) (K. Szilas).



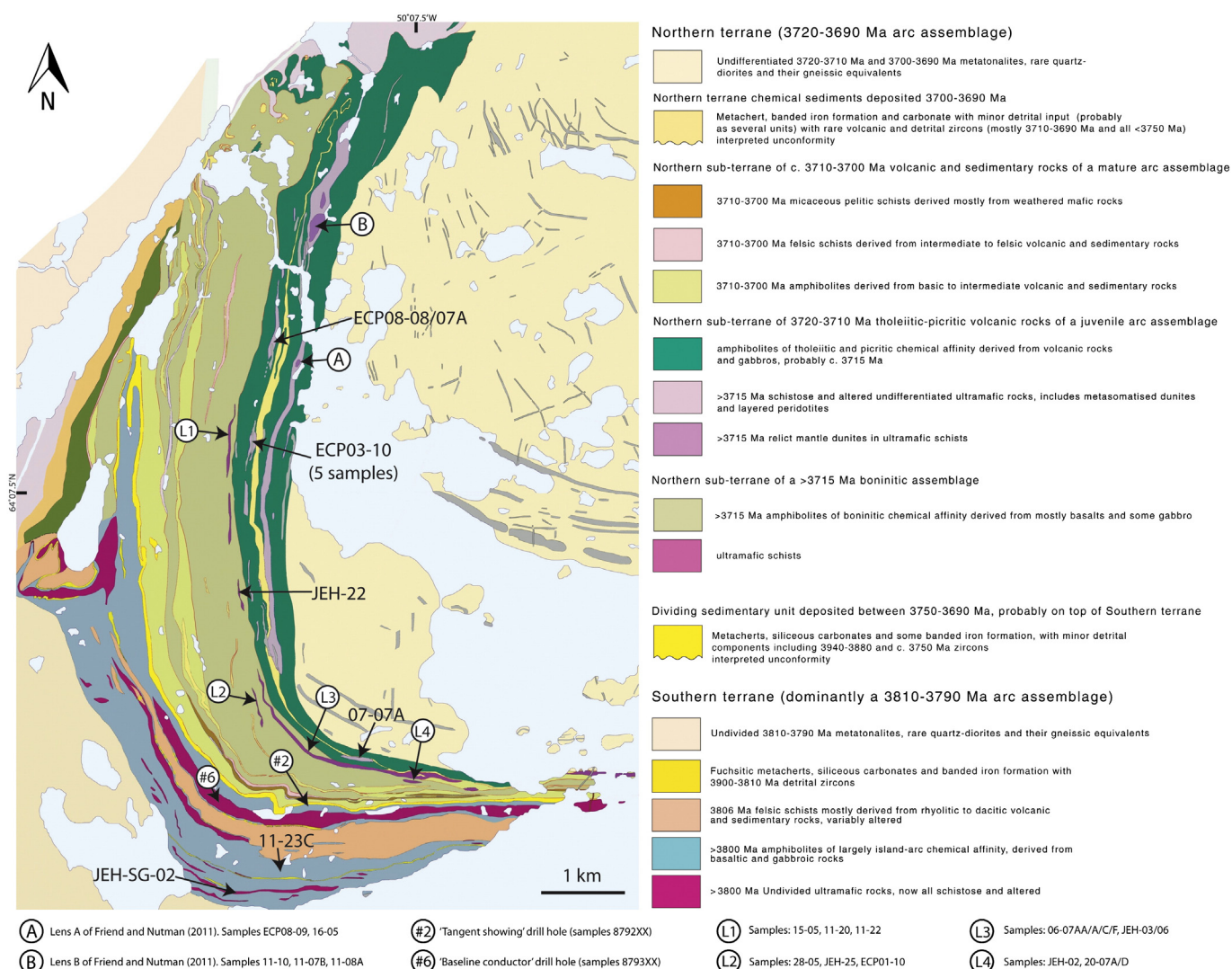


**Fig. 2.** Simplified geological map of the western arm of the Isua supracrustal belt with the sample positions marked by arrows. See Nutman and Friend (2009) for the original fully detailed geological map with U–Pb zircon ages and structural information.

(3) highly metasomatised alteration products. We demonstrate that the geochemical compositions of the ultramafic rocks in the Isua supracrustal belt are consistent with a cumulate origin. The protoliths formed by fractional crystallisation of mafic tholeiitic and boninitic magmas and subsequent accumulation of olivine, spinel and plagioclase. These cumulates then interacted with the evolving liquids to produce abundant orthopyroxene and enrichment of incompatible trace elements. This resulted in harzburgite cumulate rocks, which were subsequently hydrated and metamorphosed to form the current ultramafic assemblages observed in the Isua supracrustal belt.

## 2. Regional geology

The Nuuk region of southern West Greenland represents the amalgamation of several discrete crustal terranes, which record distinct tectonomagmatic histories (Friend et al., 1988; Nutman et al., 1996, 2004; Friend and Nutman, 2005a). Orthogneisses of the tonalite–trondhjemite–granodiorite (TTG) suite comprise the main portion of the crust in this region, but abundant supracrustal belts and anorthosite complexes are also present and are intruded by late stage granites (Fig. 1). Recently, it has been shown that the regional TTG crust was

derived by partial melting of tholeiitic basalts of similar chemical and isotope compositions as those found in the local supracrustal belts (Hoffmann et al., 2011; Næraa et al., 2012; Nagel et al., 2012; Huang et al., 2013; Hoffmann et al., 2014). This is consistent with the interpretation that the Nuuk region formed by accretionary processes similar to those observed at modern convergent margins (Nutman et al., 2007; Nutman and Friend, 2007b; Nutman et al., 2009a; Windley and Garde, 2009; Dziggel et al., 2014; Szilas et al., 2014c).

With an age of over 3.7 Ga, the Isua supracrustal belt represents one of the oldest identified assemblages of volcanic and sedimentary rocks on Earth (Moorbath et al., 1972, 1973). These rocks are situated within the Eoarchean Itsaq Gneiss Complex in the Nuuk region (Fig. 1; Nutman et al., 1996; Friend and Nutman, 2005b). They include a variety of lithologies such as mafic to felsic volcanics with pillow lava and breccia structures, gabbros, cherts, banded iron formation and clastic sediments (Appel et al., 1998; Myers, 2001; Bolhar et al., 2004; Kamber et al., 2005).

The first investigations of the Isua supracrustal belt were made by the mineral exploration company Kryolitelskabet Øresund A/S in the 1960s and were focused on the iron ore resources associated with the banded iron formation in the eastern arm of the belt. This work included

**Fig. 1.** Geological map of the Nuuk region with the western arm of the Isua supracrustal belt outlined by the red box. Based on mapping and compilation by the Geological Survey of Denmark and Greenland (GEUS).

mapping and the initial interpretation that the supracrustal rocks were autochthonous and deposited conformably onto a granitoid gneiss basement (Kurki and Keto, 1966; Keto and Kurki, 1967; Keto, 1970). Geochronology by Moorbath et al. (1972, 1973, 1977) showed that the orthogneisses at Isua are Eoarchaeon and it was observed that at least some of these form intrusive sheets within the supracrustal rocks. These therefore provided a minimum age for the supracrustal rocks and showed that the latter were in fact not deposited onto a crustal basement, but rather predated the regional crust. New mapping of the Isua supracrustal belt was done by the Geological Survey of Greenland (GGU) in the 1970s (Allaart, 1976) and yet another detailed mapping effort was completed by Nutman (1986). In the 1990s further work by GGU resulted in the interpretation that the Isua supracrustal belt resembles a Mesozoic accretionary complex based on the lithological associations (Maruyama et al., 1992; Komiya et al., 1999). Hanmer and Greene (2002) proposed a similar setting from their structural observations.

The latest and by far the most accurate map of the Isua supracrustal belt was recently published by Nutman and Friend (2009), building on years of field observations in combination with extensive zircon U–Pb age dating (e.g., Nutman et al., 1996, 1997, 1999, 2002, 2007, 2009b). Nutman and Friend (2009) provided a comprehensive synthesis of the geology of the Isua supracrustal belt, as well as a detailed map, which we have reproduced in a simplified version in Fig. 2. Below we outline the current understanding of the tectonic and metamorphic evolution of the Isua supracrustal belt and refer the reader to Nutman and Friend (2009) for a more detailed description and further literature references.

The above-mentioned authors infer that the Isua supracrustal belt represents a composite of two distinct metavolcanic to metasedimentary assemblages: (1) the ca. 3800 Ma southern terrane, and (2) the ca. 3700 Ma northern terrane. The southern terrane was previously termed 'Outer Arc Domain' and the northern terrane was termed 'Inner Arc Domain and Central Arc Domain' by Polat and Hofmann (2003). The southern and northern terranes are separated by a tectonic divide, which consists of highly sheared felsic schists with detrital zircon ages of 3940–3750 Ma (Nutman and Friend, 2009). The two terranes were juxtaposed before 3660 Ma, because they are both intruded by the so-called Inaluk dykes (Crowley, 2003). The Isua supracrustal belt shows evidence of variable metamorphic conditions, attesting to an intricate P–T–t evolution (Boak and Dymek, 1982; Rollinson, 2002, 2003), but most domains have never been above amphibolite facies conditions (ca. 610 °C and 6 kbar). At least two distinct metamorphic events affected the Isua supracrustal belt at 3610 Ma and 3550 Ma (Blichert-Toft and Frei, 2001; Nutman et al., 2002; Crowley, 2003).

Several detailed isotope studies have been conducted on rocks from the Isua supracrustal belt, which confirm its ancient age, but also its complex history of multiple metamorphic events and hydrothermal alteration overprinting (Moorbath et al., 1975; Bennett et al., 1993; Moorbath et al., 1997; Frei et al., 1999; Frei and Rosing, 2001; Bennett et al., 2002; Frei et al., 2002; Frei and Jensen, 2003; Frei et al., 2004; Hoffmann et al., 2010, 2011). Early differentiation of the mantle source for the volcanic rocks of the Isua supracrustal belt is evident from fractionation of the short-lived  $^{142}\text{Nd}$  isotope system (Boyett et al., 2003; Caro et al., 2003; Bennett et al., 2007; Rizo et al., 2013). Fractionation of the short-lived  $^{182}\text{W}$  isotope system has also been documented, but the meaning of this anomaly remains unclear, as it can be affected by late meteorite input (Schoenberg et al., 2002; Izuka et al., 2010; Willbold et al., 2011) or even hydrothermal alteration (Touboul et al., 2014).

The ultramafic rocks of the Isua supracrustal belt, which are the main focus of the present study, are commonly affected by carbonation (Rose et al., 1996). An important observation is that some of the ultramafic rocks display uninterrupted transitions into gabbros in certain areas of the Isua supracrustal belt (Nutman et al., 1996). The origin of the ultramafic rocks has been suggested to be anything from extensively metasomatised alteration products to komatiites, cumulates or mantle

residues (Allaart, 1976; Dymek et al., 1988a, 1988b; Rosing, 1989; Rosing et al., 1996; Rollinson, 2007; Friend and Nutman, 2010, 2011). In this study we specifically test these different hypotheses, using new geochemical data obtained on the largest sample collection of ultramafic rocks from the Isua supracrustal belt to date.

### 3. Samples and petrography

In this study we present new geochemical data for 52 samples from the Isua supracrustal belt of mainly ultramafic composition (amphibolites and serpentinites with MgO ranging from 9.7 to 49.0 wt.%). These samples are all from the western arm of the Isua supracrustal belt, and rocks from the Inner, Central and Outer assemblages are represented. Of these samples, 21 are from two drill cores taken in the southern portion of the western arm, whereas the remaining 31 samples are surface samples. Some of the surface samples have previously been used in a study of hydrogen and oxygen isotope compositions of the Isua serpentinites by Pope et al. (2012). The drill core material was provided by the mineral exploration company NunaMinerals A/S. One drill core is from the so-called 'Tangent Showing' (Isua 08-#2) with azimuth 260° and dip 60°. The other drill core is from the so-called 'Baseline Conductor' (Isua 08-#6) with azimuth 350° and dip 55° (see positions in Fig. 2). Each drill core sample is ca. 20 cm in length, but only 10 cm sections were powdered from each individual sample for the geochemical analysis. The drill core samples appear homogeneous without any notable variation in modal composition at the scale of the individual samples. The surface samples were cut by a diamond saw to remove weathered crusts. Thin sections were prepared for a representative selection of the different rock types and these were examined by polarised microscopy and further by electron microprobe (see Section 5.3 and Table 5).

In general the samples can be divided into serpentinites and amphibolites. The serpentinites are usually massive and homogeneous, but can also have significant schistosity and crenulation foliation (Fig. 3a, b and d). They mainly comprise serpentine, talc and oxide minerals. Some of the serpentinites also contain metamorphic olivine grains, which are commonly distributed in patches that are surrounded by serpentine and olivine is sometimes rimmed by magnetite (Fig. 3a and b). Titanian chondrodite and clinohumite has been reported in these serpentinites by Dymek et al. (1988b).

The amphibolites are usually foliated with oriented growth of elongate amphiboles, which range in colour from dark green to grey and light brown. Amphiboles are either of rhomb-shaped euhedral shape or consist of aggregates of elongated needles (Fig. 3c, e and f). The compositions of the amphiboles are variable and reflect their host rock and range from tremolite to cummingtonite to anthophyllite. Usually, less than 10% orthopyroxene is found in these rocks, but they commonly have large amounts of normative orthopyroxene (up to 79%) due to their relatively high  $\text{SiO}_2$  and  $\text{Al}_2\text{O}_3$  contents (see Section 5.1). So-called garbenschiefer texture, consisting of amphibole aggregates, is visible in hand samples from the central assemblage (boninitic sequence).

### 4. Methods

We have acquired major and trace element data by ICP methods from ACME Labs, Vancouver (see Supplementary Table 1) and reanalysed several samples for their trace element contents at Lamont-Doherty Earth Observatory, New York (Supplementary Table 2). We have calculated the normative compositions of the samples following the procedures of Kelemen et al. (1992, 1998) (Supplementary Table 3). Platinum-group element data (available in Supplementary Table 4) were obtained at Université du Québec à Chicoutimi by NiS-FA pre-concentration and measured by MC-ICP-MS following the procedures of Savard et al. (2010). Electron microprobe analysis of minerals was conducted at the Museum of Natural History, New York (representative data are presented in Supplementary Table 5). The reader is referred to the online Appendix A for a detailed description of the analytical procedures. All samples

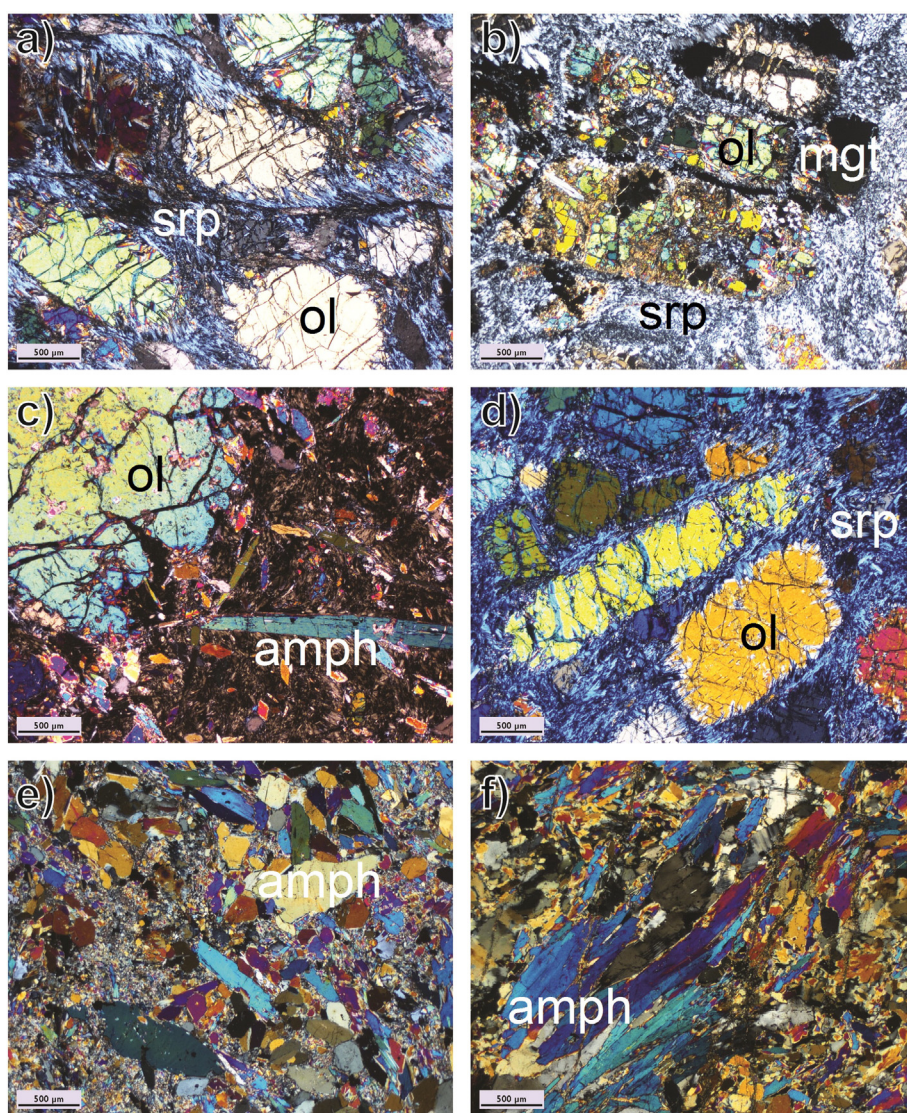


**Fig. 3.** Microphotographs of Isua lithologies. a) Basalt cumulate sample 16-05 from the inner sequence showing large olivine porphyroblasts that are evenly distributed and surrounded by a matrix of sheared serpentine. This sample is from the Lens A of Friend and Nutman (2011). b) Basalt cumulate sample 11-10 (from Lens B) shows disrupted olivine grains that are rimmed by magnetite. The exsolution of Fe-rich oxides is consistent with the elevated Mg-contents of these olivine grains (Mg# of 94–98). c) Boninite cumulate sample ECP01-10 with large olivine in the upper left corner and both rhomb-shaped and elongate amphiboles. d) Boninite cumulate sample ECP08-09 showing elongate olivine grains in a matrix of serpentine. e) Tholeiitic basalt sample 879335 with various subhedral amphiboles. f) Isua boninite sample 879346 from the central sequence showing amphibole fibrolite and abundant plagioclase as suggested by the elevated  $\text{Al}_2\text{O}_3$  content of these rocks. All of the microphotographs were taken with crossed polarisers. Please note that some of the colour variation may be due to different automatic adjustments by the software, which may not accurately reproduce the true colours as seen in the microscope. (For interpretation of the references to colour in this figure legend, the reader is referred to the web version of this article.)

are described on a volatile-free basis in the following and diagrams were plotted with the freeware program GCDKit by Janosek et al. (2006). We present supplementary geochemical figures in Appendix B and use the prefix 'B' when referring to these.

## 5. Results

### 5.1. Major and trace element data

Two distinctly different magmatic trends have been identified in the Isua supracrustal belt by previous workers: (1) a tholeiitic basalt fractionation series that has slightly enriched incompatible trace element patterns (e.g., Polat et al., 2003; Jenner et al., 2009), and (2) a boninite-like fractionation series, which has depleted incompatible trace element abundances (Polat et al., 2002). These two contrasting igneous suites can easily be distinguished by plotting their  $\text{Al}_2\text{O}_3/\text{TiO}_2$  ratios (Fig. 4) and by plotting e.g.  $\text{Al}_2\text{O}_3$ ,  $\text{TiO}_2$ , La, Nb, Zr and Th vs.

MgO (Fig. 5), or by their primitive mantle (PM) normalised trace element patterns (Fig. 6). The samples in this study with less than about 20 wt.% MgO have compositions that overlap with previously published data for Isua volcanic rocks. Accordingly, we have therefore classified these samples as either tholeiites or boninites (Figs. 5 and 6). There appears to be a gap in MgO contents between ca. 20 to 27 wt.% in our sample collection. Although it is possible that this discontinuity is an artefact of the sampling, we treat the samples with more than 27 wt.% MgO as a separate group. These ultramafic samples also appear to follow the two distinct fractionation trends, one plot towards the tholeiites and the other towards the boninites (Fig. 5). Therefore, they are divided into basalt- and boninite-affinity trends as seen in Fig. 4. The ultramafic rocks are dominated by olivine (up to 94%), orthopyroxene (up to 79%), some plagioclase (up to 25%) and minor clinopyroxene (up to 15%) in their normative mineralogy (Fig. B1 and Table 3).

The tholeiitic basalt samples in our collection ( $n = 4$ ) have relatively high  $\text{SiO}_2$  (51.6–52.9 wt.%),  $\text{TiO}_2$  (0.69–0.82 wt.%), and FeO

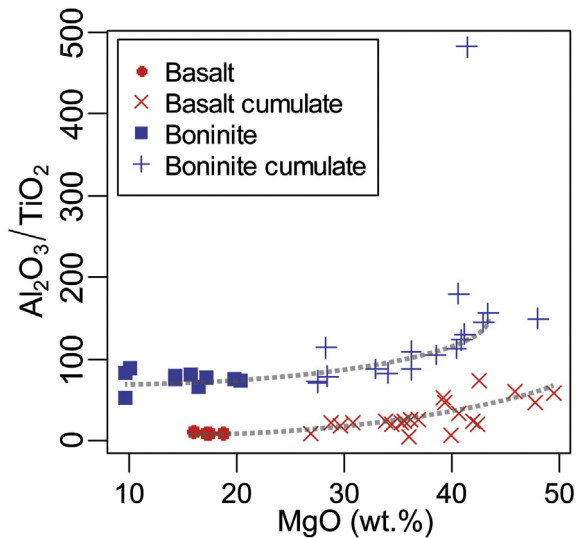


**Fig. 4.** The tholeiitic and the boninitic magmatic trends can effectively be distinguished by their  $\text{Al}_2\text{O}_3/\text{TiO}_2$  ratio versus MgO content and these have been used to classify the ultramafic rocks, which are otherwise difficult to separate based on their absolute trace element abundances.

(11.4–12.9 wt.%), and low  $\text{Al}_2\text{O}_3$  (6.9–9.0 wt.%). These samples have MgO content ranging from 16.0 to 18.8 wt.%. Their  $\text{CaO}/\text{Al}_2\text{O}_3$  ratios are 0.8–1.0 and their  $\text{Al}_2\text{O}_3/\text{TiO}_2$  ratios range from 10 to 11. Their chondrite-normalised rare earth element (REE) patterns (Fig. B2) are

slightly enriched with  $\text{La}_{\text{CN}}/\text{Yb}_{\text{CN}}$  of 3.7–5.4 and they have minor negative Eu-anomalies ( $\text{Eu}/\text{Eu}^*$  of 0.7–1.0). Their primitive mantle-normalised (PM) trace element patterns show minor negative anomalies for Ta, Nb, and Ti, and two samples have significantly negative Sr-anomalies. Positive anomalies are observed for Pb, and Th is elevated at about 20x PM-value (Fig. 6).

The boninite-like samples ( $n = 10$ ) are characterised by having high  $\text{Al}_2\text{O}_3$  (14.2–20.0 wt.%), less  $\text{SiO}_2$  than the tholeiitic samples (46.1–51.1 wt.%), and low FeOt (7.52–10.5 wt.%) and  $\text{TiO}_2$  (0.13–0.35 wt.%). Their MgO contents range from 9.68 to 20.5 wt.%. Their  $\text{CaO}/\text{Al}_2\text{O}_3$  ratios are 0.3–0.8 and their  $\text{Al}_2\text{O}_3/\text{TiO}_2$  ratios range from 53 to 89. The chondrite-normalised REE patterns of the boninite-like samples are depleted with  $\text{La}_{\text{CN}}/\text{Yb}_{\text{CN}}$  of 0.2–0.5 and they have variable Eu-anomalies of 0.7–1.9. Their PM-normalised trace element patterns show distinct positive anomalies for Pb, Sr and Hf (Fig. 6).

The ultramafic samples ( $n = 38$ ) have MgO contents of 27.0–49.4 wt.% and high, but variable, FeOt contents ranging from 7.51 to 16.5 wt.%. There are negative correlations between MgO and  $\text{SiO}_2$  (38.6–51.7 wt.%),  $\text{Al}_2\text{O}_3$  (0.61–11.1 wt.%),  $\text{CaO}$  (0.02–7.23 wt.%) and  $\text{TiO}_2$  (0.01–0.47 wt.%; with sample ECP08-07A being an outlier at 0.93 wt.%) as seen in Fig. 5. As mentioned above, the ultramafic rocks can be further divided into two distinct groups based on their apparent affinities with either the basaltic or boninitic trends. It is also possible to separate these in two groups from their  $\text{Al}_2\text{O}_3/\text{TiO}_2$  ratios as a function of MgO content (Fig. 4). This ratio effectively distinguishes between the tholeiitic basalts and the boninites, and similar trends are seen for the ultramafic rocks. The ultramafic rocks of basalt-affinity have Cr ranging from 1381 to 18,516 ppm and Ni from 90 to 3174 ppm. Their chondrite-normalised  $\text{La}_{\text{CN}}/\text{Yb}_{\text{CN}}$  ratios are variable at 0.1–2.5 and they

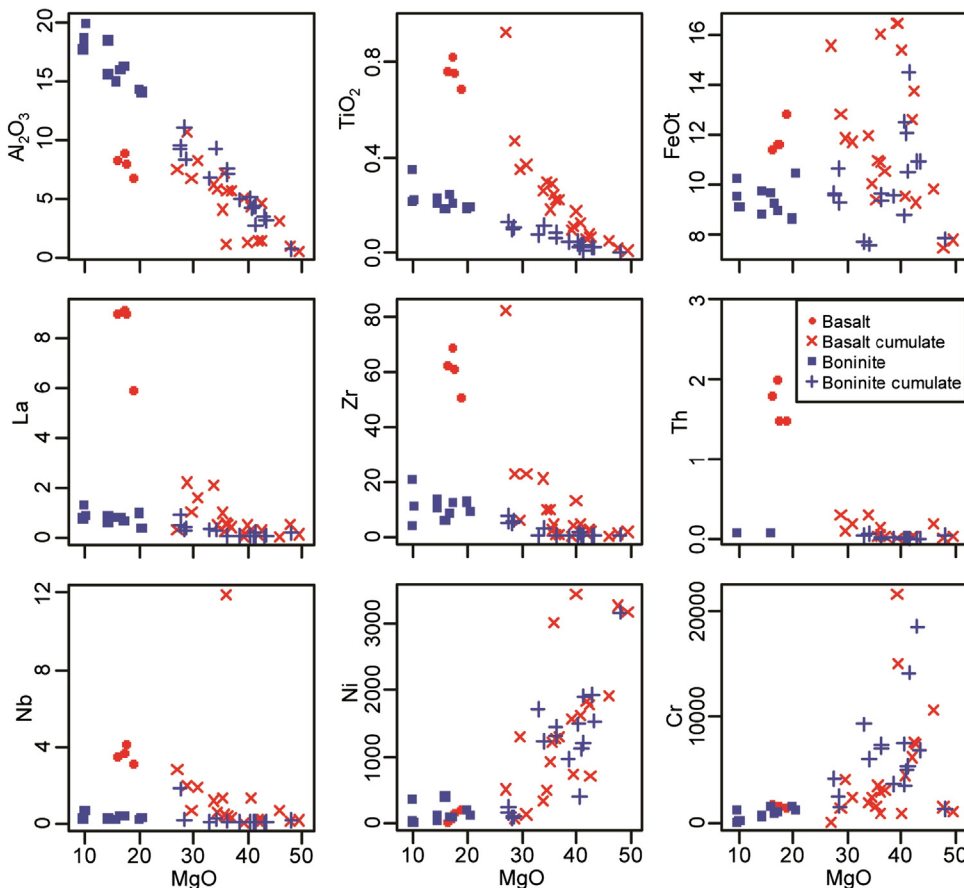


**Fig. 5.** Variation diagram for the Isua data presented in this study, showing  $\text{Al}_2\text{O}_3$ ,  $\text{TiO}_2$ , La, Nb, Zr and Th vs. MgO (oxides are in wt.% and trace elements are in ppm). Note the distinctly different tholeiitic and boninitic compositions and the tendency for the ultramafic rocks to follow either of these trends as a function of MgO contents. The outlier in the  $\text{TiO}_2$  and the Zr plots is sample ECP08-07A and the outlier in the Nb plot is sample 07-07A. These elevated values likely reflect accumulation of HFSE-rich accessory phases, such as ilmenite, rutile or titanoclinohumite.

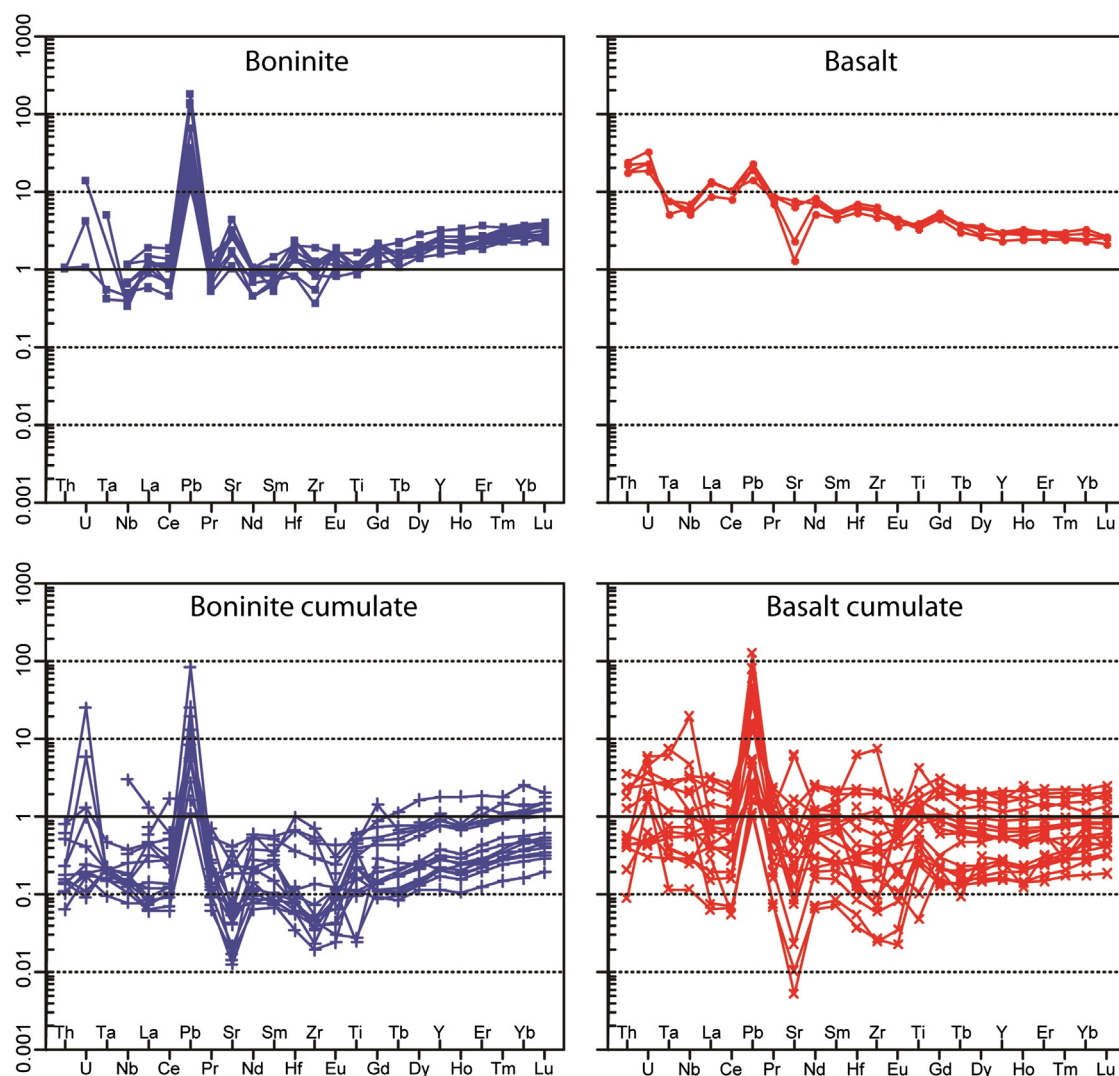


**Fig. 6.** Primitive mantle-normalised trace element diagram for the Isua data presented in this study. PM values from [Palme and O'Neill \(2003\)](#). Note the overall depleted patterns of the boninites and the slightly enriched patterns of the basalts.

have negative Eu-anomalies (0.2–1.0) with one outlier at 1.5 (sample 879246). They have strongly positive Pb-anomalies and mostly negative Sr-anomalies (Fig. 6). The ultramafic rocks of boninite-affinity ( $n = 17$ ) have Cr ranging from 1381 to 18,516 ppm and Ni from 90 to 3174 ppm. Their chondrite-normalised  $La_{CN}/Yb_{CN}$  ratios are variable at 0.1–3.0 and they have consistently negative Eu-anomalies (0.2–0.8). They also have strongly positive Pb-anomalies and mostly negative Sr-anomalies (Fig. 6).

### 5.2. Platinum-group element data

The chondrite-normalised platinum-group element (PGE) patterns are fractionated with positive slopes for most of the Isua rocks (Fig. 7). The Os and Ir contents are relatively low in all of the samples and Ru and Rh abundances are moderately high. Pt and Pd are mostly elevated, except for some of the ultramafic rocks that are depleted in Pt and Pd, and thus their PGE patterns have a hump at Ru and Rh. The PGE data are available in Supplementary Table 4.

### 5.3. Electron microprobe data

Basalt cumulate sample 16-05 from Lens A of [Friend and Nutman \(2011\)](#) has olivine Mg# (100 × molar  $Mg/[Mg + Fe^{2+}]$ ) ranging from 88.4 to 90.9 and NiO from 0.43 to 0.62 wt.%. This sample is the only

one in our collection that has significant amounts of spinel. The spinel is chromite with Mg# ranging from 5.9 to 23.2, Cr# (100 × molar  $Cr/[Cr + Al]$ ) from 72.4 to 99.3 and  $Fe^{3+}\#$  (100 × molar  $Fe^{3+}/[Fe^{3+} + Al + Cr]$ ) from 6.1 to 39.3 (see Supplementary Table 5).

Basalt cumulate sample 11-10 (from Lens B in Fig. 2) has olivine with Mg# of 94.2 to 98.3 and NiO from 0.38 to 0.69 wt.%. This sample has very little spinel (4 out of 52 measured oxide grains) and oxides are mainly pure magnetite. The few grains of spinel that we found had Mg# from 26.2 to 47.9, Cr# from 72.0 to 99.5 and  $Fe^{3+}\#$  from 6.2 to 34.9.

Boninite cumulate sample ECP08-09 has olivine with a rather tight range of Mg# from 88.3 to 91.1 and NiO from 0.45 to 0.60 wt.%. We did not find any spinel in this sample and all oxides were magnetite and ilmenite.

Boninite cumulate sample ECP01-10 has the lowest olivine Mg#s that we found in this study ranging from 77.6 to 81.5 and also the lowest NiO from 0.20 to 0.29 wt.%. In this sample we found mainly ilmenite and some magnetite.

Fig. 8a shows the olivine compositions with their NiO contents as a function of Mg#. Fig. 8b shows the Cr# vs. Mg# of the spinels with the round symbols being the samples with  $Fe^{3+}\#$  less than 10, which are likely to represent primary compositions, whereas elevated  $Fe^{3+}\#$  (crosses) likely reflect metamorphic resetting (e.g., [Bernstein et al., 2013](#)). We also note that Cr# is positively correlated with  $TiO_2$  in the spinel in the samples that have  $Fe^{3+}\#$  over 10 (Fig. B3). Olivine is

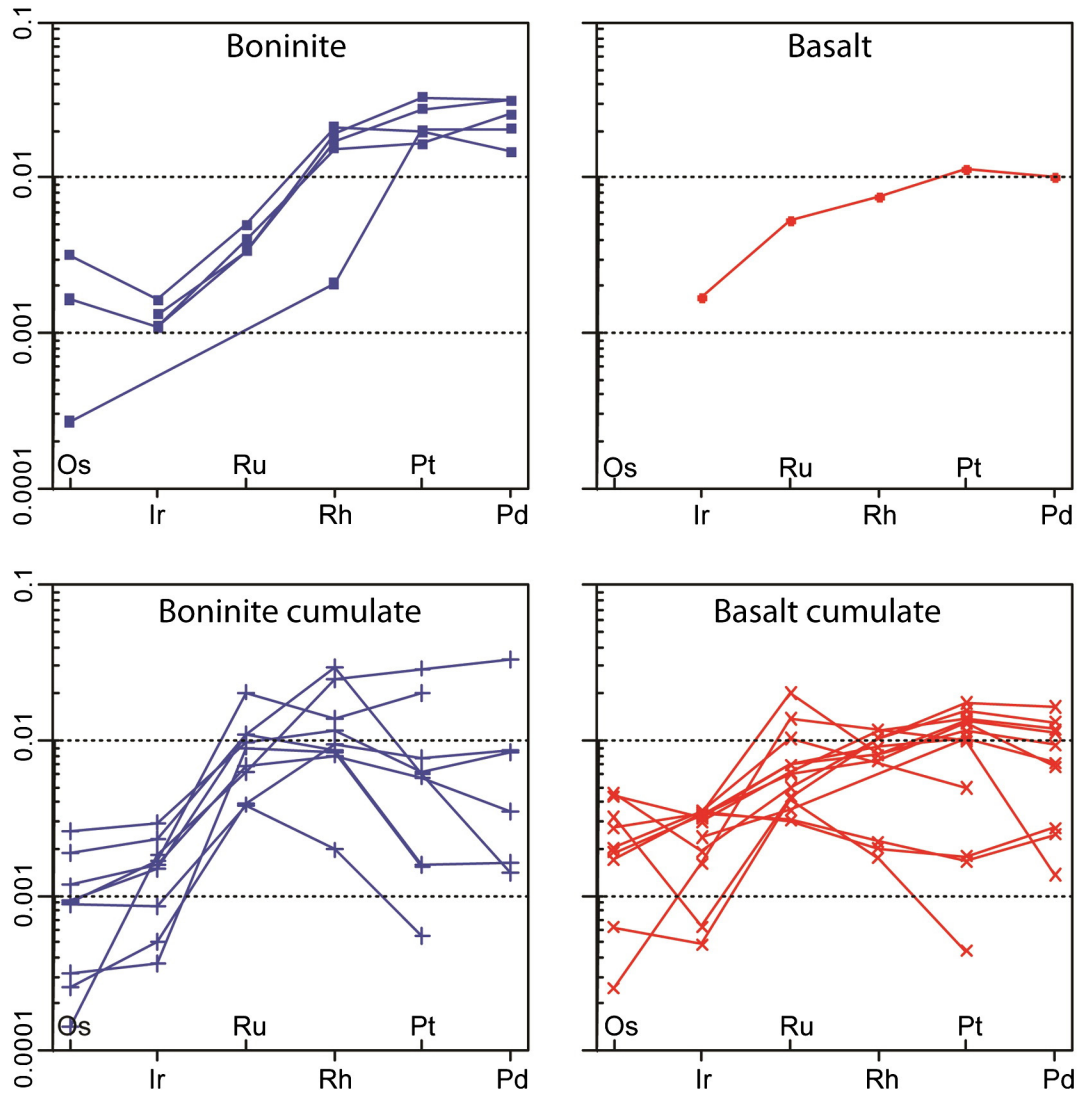


Fig. 7. Chondrite-normalised (Fisher-Gödde et al., 2010) platinum-group element patterns for the Isua basalts, boninites and ultramafic rocks presented in this study. Note the depleted Os and Ir abundances, which are significantly lower than mantle residues, which typically have values at about  $0.01 \times$  chondrite.

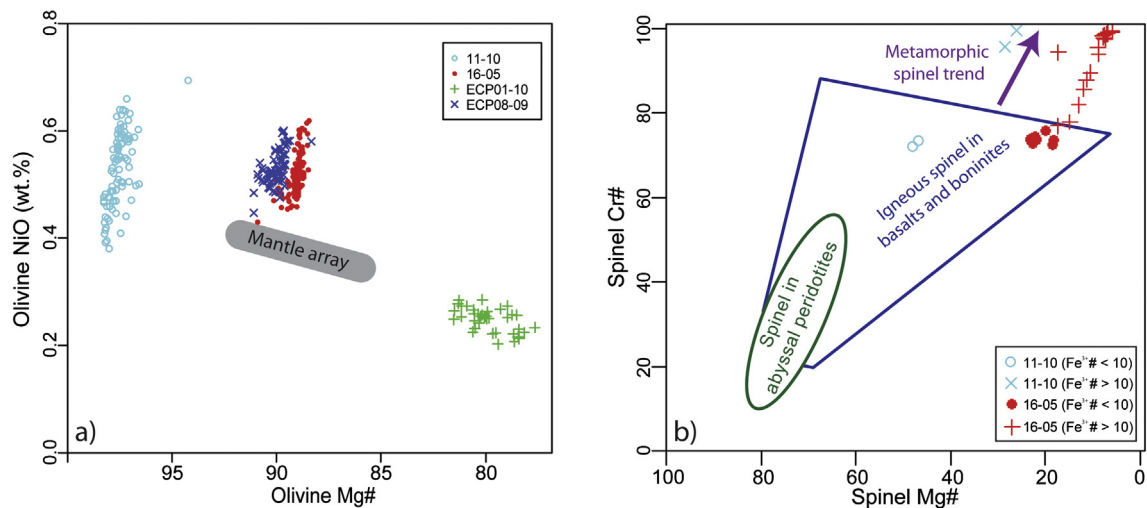


Fig. 8. a) NiO vs. Mg# in olivine. Mantle array from Takahashi et al. (1987). b) Cr# vs. Mg# in spinel. Abyssal mantle spinel field from Dick and Bullen (1984) and igneous field of basalts and boninites from Barnes and Roeder (2001). Samples 16-05 and 11-10 are basalt cumulates from Lenses A and B, respectively, whereas samples ECP08-09 and ECP01-10 are boninite cumulates from Lens A and Locality 2 in the central boninite sequence, respectively (Fig. 2).

generally homogeneous and unzoned, but rare examples have rims, which are slightly more fosteritic. For example, sample ECP01-10 had one olivine grain with Mg# of 78.5 in the core and Mg# of 81.2 at the rim. The few spinel grains that were observed commonly have cores with relatively low Cr# and high Mg#, but rims with increasingly elevated Cr# and decreasing Mg#, consistent with magnetite (magnesiocromite) replacement, as seen in Fig. 8b for sample 16-05.

## 6. Discussion

### 6.1. Assessment of post-magmatic element mobility

Ultramafic rocks are susceptible to alteration of their primary igneous compositions due to the limited stability of olivine and pyroxenes at low pressures and hydrous conditions. It is relevant to consider this for the Isua supracrustal belt, because it has been documented that these rocks have experienced early seafloor alteration, as well as multiple events of metamorphism (Rollinson, 2002; Polat and Hofmann, 2003; Polat et al., 2003; Nutman and Friend, 2009). Thus, care must be taken when interpreting the petrogenesis of these ultramafic rocks, as extensively metasomatic alteration has been documented in supracrustal belts elsewhere in the Nuuk region (e.g., Ordóñez-Calderón et al., 2008; Szilas and Garde, 2013). In higher grade metamorphic rocks of the Itsaq gneiss complex, partial melting and melt depletion may even disturb high field strength elements (HFSE) in supracrustal rocks (e.g., Szilas et al., 2014a). However, the Isua supracrustal belt never reached granulite facies metamorphic conditions and HFSE consistently show coherent variation with each other, and even with potentially mobile components such as MgO (Fig. 5).

It has been proposed that the ultramafic rocks at Isua are heavily altered by carbonate-rich fluids which supposedly introduced Al in the most strongly metasomatised rocks (Rosing, 1989; Rosing and Rose, 1993). However, although the ultramafic rocks have clearly been carbonated, the systematic correlations of major and trace elements in our data are consistent with igneous fractionation trends (Fig. 5). The volatile content (LOI) is not correlated with Al or any other major elements. Furthermore, we carried out isocon-modelling following Gresens (1967) and Grant (1986) of adjacent ultramafic samples, which results in a wide scatter of elements that are usually considered immobile, and thus metasomatic alteration is not a viable explanation for the compositional variation observed in the ultramafic rocks in this study. The observed geochemical variation is in fact better explained by fractional crystallisation in combination with cumulate–liquid interaction, which we will demonstrate in the following sections.

Serpentinisation during rock–seawater reaction commonly results in elevated large ion lithophile elements (LILE) and LREE (resulting in positive Eu anomalies), as well as enrichment in carbonate-hosted trace elements (Pb and Sr) when accompanied by carbonation (Niu, 2004; Paulick et al., 2006; Kodolányi et al., 2012; Marchesi et al., 2013a). MgO can either be added or lost depending on the conditions at which the serpentinisation occurs, but usually MgO-changes are small (Snow and Dick, 1995; Deschamps et al., 2013). Similar element mobilities are observed during high-temperature serpentinisation by crustal-derived fluids (Liu et al., 2008; Xie et al., 2013). The negative Sr- and Eu-anomalies in the Isua ultramafic rocks could either be caused by alteration or plagioclase fractionation under reducing conditions.

Although certain fluid-mobile components (e.g., Ca, K, Na, Rb, Ba, and Sr) may have been redistributed in these rocks, the more immobile components (e.g., Al, Ti, Zr, Nb, and Th) are unlikely to have been significantly affected by alteration. With the exception of U, Pb, Sr, and Eu, we consider that the elements whose concentrations are presented in Figs. 5 and 6 preserved their primary magmatic abundances and can be related to fractional crystallisation processes, as also suggested by Polat and Hofmann (2003). Given that the trace element abundances are rather low in these ultramafic rocks, with several elements below their detection limits, we have to be careful not to over-interpret the

geochemical features that are seen in the trace element diagrams (Fig. 6). Nevertheless, the two groups of ultramafic rocks have broadly similar patterns as those in the corresponding mafic rocks, which suggests that they may represent two distinct magmatic suites.

### 6.2. Major and trace element signatures

Our new geochemical data for the mafic rocks are consistent with the two previously documented contrasting volcanic suites in the Isua supracrustal belt, namely a boninite-like series (Polat et al., 2002) and a tholeiitic basalt series (e.g., Polat et al., 2003; Jenner et al., 2009). These two suites have distinct chemical variation trends that are particularly obvious when plotting  $\text{Al}_2\text{O}_3$ ,  $\text{TiO}_2$ , La, Nb, Zr and Th vs. MgO (Figs. 4 and 5). A subduction zone setting for the Isua volcanic rocks appears likely due to the presence of basalts with HFSE depletion and rocks of boninitic affinity, as also noted by previous authors (e.g., Polat et al., 2002; Jenner et al., 2009). The depleted trace element patterns of the boninite-like rocks are consistent with previous melt depletion of their mantle source, which is supported by their highly elevated Hf-isotope compositions (Hoffmann et al., 2010). Similar boninite-like rocks are also found in the 2.7 Ga Abitibi greenstone belt in Canada (Kerrich et al., 1998) and they show a complete overlap with the Isua boninite-like suite in terms of both major and trace element compositions.

Friend and Nutman (2011) proposed that the most depleted Isua ultramafic rocks (in particular from Lenses A and B in Fig. 2), may represent dunitic sub-arc mantle. Therefore, to test this model, we have compared the Isua rocks with published data on mantle residues from forearc settings, such as the active Mariana arc and the obducted Oman ophiolite (see Appendix B, Figs. B4–B7). In terms of major elements there is some overlap for certain elements, but FeO<sub>t</sub> is significantly higher in the Isua rocks, and the trace element concentrations in mantle residues are more depleted than any of the samples from the Isua supracrustal belt.

Potential Eoarchaean mantle residues in the Itsaq Gneiss Complex south of the Isua supracrustal belt have previously been investigated (Bennett et al., 2002; Friend et al., 2002; Rollinson et al., 2002), but these are associated with layered intrusive complexes and appear to be geochemically different from the ultramafic rocks in the Isua supracrustal belt (Rollinson, 2007).

Although the geochemical compositions of the ultramafic rocks at Isua are distinct from mantle residues, it should be mentioned that the uppermost mantle portion below oceanic crust can become modified by reaction with percolating melts to form dunite, which is a commonly observed feature of ophiolites (e.g., Kelemen et al., 1992; Takazawa et al., 1992; Bédard et al., 1998; Kelemen et al., 2003; Garrido et al., 2007; Marchesi et al., 2009). However, this process does not cause enrichment of FeO<sub>t</sub> and SiO<sub>2</sub> to the levels that we observe for the Isua rocks and would not explain the consistent variation trends in the Isua data (Figs. 5 and B6–7). The highly fractionated PGE and Fe-rich spinel compositions that we have reported on the ultramafic rocks at Isua are also not consistent with a melt-modified mantle origin of these rocks (see Sections 6.3 and 6.4). Furthermore, there is no evidence of the unmodified harzburgitic mantle residues within which such dunites are formed.

We have also compared the Isua rocks with the komatiite database of Fiorentini et al. (2011) (Figs. B8–9). The boninite-like lavas from Isua are distinctly different from komatiites. In particular, the Isua suite has significantly higher  $\text{Al}_2\text{O}_3$  and lower  $\text{TiO}_2$ . The ultramafic rocks are much more Fe- and Al-rich than komatiites. As mentioned previously, the boninite-like Isua suite is virtually identical to rocks from the Abitibi belt, which were also interpreted to represent boninites (Kerrich et al., 1998). Thus, the bulk-rock compositions of the ultramafic rocks in the western arm of the Isua supracrustal belt are not similar to komatiites, as also concluded by previous work (Jensen, 2002; Polat et al., 2002). In particular the very high  $\text{Al}_2\text{O}_3/\text{TiO}_2$  ratios are not

known from any komatiites, whereas Phanerozoic boninites have ratios that overlap with those of the boninite-like rocks in the Isua supracrustal belt.

The Isua tholeiitic basalts have vague resemblance with “Karasjok-type” komatiites, but have significantly higher  $\text{Al}_2\text{O}_3$  contents. Besides, primary komatiite liquids have MgO ranging from 18 to 30 wt.% (Arndt et al., 2008), whereas the most likely candidate for a primitive Isua tholeiitic basalt without olivine accumulation likely has a MgO contents of around 12 wt.% and the primary boninite would have about 16 wt.%, based on the observed major element variation. Additionally, the corresponding Isua cumulates are again much more Fe- and Al-rich and as we will show in Section 6.5, the composition of these agree well with the calculated fractionating assemblage in combination with cumulate–liquid interaction.

It has been proposed in many studies that the Isua supracrustal belt represents an arc-related sequence of rocks (e.g., Furnes et al., 2009; Friend and Nutman, 2010) and we have therefore compared our new data for Isua with data from the Mesozoic Kohistan (Figs. B10–11) and Talkeetna island arc sections. Despite minor discrepancies, the data show overall similar trends – particularly for the boninite-like Isua suite, so our data are broadly consistent with an arc origin for this suite.

Unfortunately, only limited bulk-rock data exists on dunites and harzburgites of cumulate origin. However, mantle rocks generally have FeO<sub>t</sub> contents of about 7 wt.%, whereas ultramafic cumulates can have FeO<sub>t</sub> levels twice as high, as also observed for the Isua rocks. This difference between mantle and cumulate peridotites is supported by the global serpentinite database of Deschamps et al. (2013), which is dominated by mantle-derived rocks in which Fe-rich serpentinites are relatively rare (Fig. B12). In contrast, cumulate peridotites are commonly Fe-rich with values within the range we observe for the Isua ultramafic rocks (e.g., Nielsen, 1981; Johnson et al., 2004; Liu et al., 2008; Thakurta et al., 2008; Jagoutz and Schmidt, 2013). We also note similarities between the Isua boninite cumulates and ultramafic cumulates from Pohorje in Slovenia (De Hoog et al., 2011), which were interpreted to have plagioclase–peridotite protoliths.

### 6.3. Platinum-group element patterns

Platinum-group elements (PGEs) remain largely immobile during alteration and metamorphism (e.g., Barnes et al., 1985; Crocket, 2000; Wang et al., 2008). Significant mobility of PGEs only occurs under strongly oxidising conditions seen during soil- and gossan-formation (Suárez et al., 2010), although Pt and Pd can potentially be lost during serpentinisation (Lorand, 1989; Alard et al., 2000; Guillot et al., 2000; Marchesi et al., 2013b). In contrast, Pt and Pd are elevated relative to other PGE in the majority of the Isua rocks. Therefore, PGEs may provide a relatively robust indicator of protolith origin for the Isua ultramafic rocks, despite early alteration and multiple metamorphic events.

Refractory alloys and monosulfide solid solution (MSS) determines the abundances of iridium-group PGEs (IPGEs: Os, Ir and Ru), which are highly compatible in mantle rocks, whereas platinum-group PGEs (PPGEs: Pt, Pd, Rd) are highly compatible in Cu–Ni-rich sulfide minerals and melts, which readily dissolve into silicate melts (Alard et al., 2000; Ballhaus et al., 2006; Luguet et al., 2007; Lorand et al., 2008). Therefore, the two groups of PGEs are fractionated in partial melts of the mantle, which results in fractionated PGE patterns with positive slopes (Barnes and Picard, 1993). Due to the strongly compatible nature of IPGEs and the moderately incompatible behaviour of PPGEs (Momme et al., 2002; Woodland et al., 2002; Bézou et al., 2005; Fiorentini et al., 2011; Peucker-Ehrenbrink et al., 2012), cumulate PGE patterns can additionally become fractionated by accumulation of PGE-rich phases. The positive Ru anomalies that we observe in some of the Isua samples are likely due to accumulation of chromite in which Ru is highly compatible (Ballhaus et al., 2006; Locmelis et al., 2011). This feature is for example observed in cumulus chromitites from Thetford Mines and Bay of Island, Canada (Escayola et al., 2011).

Mantle residues and magmatic cumulates can therefore potentially be distinguished on the basis of their Ir abundances and their general PGE patterns, because mantle rocks have flat chondrite-normalised patterns ( $\sim 0.01 \times$  chondrite), whereas magmas and their cumulates have fractionated patterns with low Or and Ir levels (Hattori and Hart, 1997; Hattori and Shirahase, 1997; Guillot et al., 2000; Hattori et al., 2010; Deschamps et al., 2013). The fractionated PGE patterns of the Isua rocks suggest a magmatic rather than a mantle origin (Fig. 7) and plot outside the abyssal mantle field in Fig. 9. The positive fractionation with low levels of Os and Ir cannot be produced by alteration of a mantle precursor, because Os and Ir are retained in refractory alloys and are therefore the least mobile PGEs. The basalt and boninites have consistently elevated Pt and Pd, whereas a few of the ultramafic rocks have low levels of Pt and Pd, which may be due to loss to the liquid or alternatively loss during serpentinisation and breakdown of sulfides. In Fig. B13 we compare our PGE data for the Isua rocks with data from fresh peridotites from Oman (Hanghøj et al., 2010). It is apparent that even melt-modified dunites of the Oman ophiolite are not as depleted in Os and Ir as the Isua ultramafic samples and that this feature is likely to be of primary origin. Overall, the PGE data provide strong evidence for the interpretation that none of the Isua rocks represent mantle residues, but that their protoliths were fractionated magmas and their derivative cumulates.

Finally, it is worth mentioning that the fractionated PGE patterns of the Isua rocks are similar to those observed in modern volcanic equivalents. This may imply that the mantle sources of the Isua basalts and boninites, which formed before 3.7 Ga, were already equilibrated with the PGE-contribution from the “late veneer”. PGE ratios in the Eoarchean mantle were therefore similar to present day Bulk Silicate Earth (Becker et al., 2006), which indicates efficient refertilisation of Earth’s mantle, with respect to highly siderophile elements, following core formation. This is in agreement with recent studies, which point to very early mixing and homogenisation of PGEs into Earth’s mantle (Dale et al., 2012; Day et al., 2012; Coggon et al., 2013).

### 6.4. Mineral compositions

The very magnesian olivine compositions (Mg# 94.2–98.3) of basalt cumulate sample 11–10 must be metamorphic (Fig. 8a). This is consistent with the observation of magnetite along the margins of these olivine grains (Fig. 3b). Almost all primary chromite has been altered to magnetite in this rock and the four chromite grains that we have found have low Mg# (26.2–47.9), indicative of low temperature Fe–Mg exchange with olivine and other silicates. Therefore, this sample

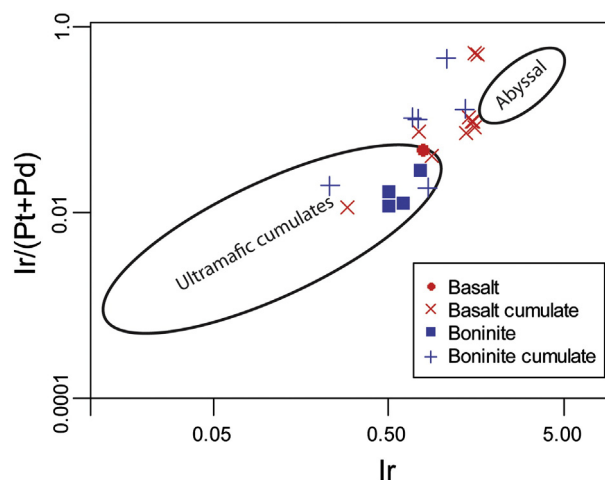


Fig. 9. The Isua PGE data plotted in a Hattori-diagram. None of the samples plot within the abyssal mantle field, which is consistent with their fractionated patterns (Fig. 6). Most of the samples plot between the mantle and cumulate fields, but some do plot within the latter. Abyssal mantle and cumulate fields from Hattori and Hart (1997) and Hattori and Shirahase (1997).

does not provide much information regarding mineral compositions in the protolith. Boninitic cumulate sample ECP01-10 on the other hand has low olivine Mg# (77.6–81.5), which fits with its relatively low bulk-rock Mg#. However, olivine would not be expected to maintain its primary composition in these rocks, which have experienced multiple phases of metamorphism, and are more likely to represent equilibration with its host rock.

Basalt cumulate sample 16-05 and boninitic cumulate sample ECP08-09 have olivine compositions with Mg# ranging from 88.3 to 91.1. Their elevated NiO-content (Fig. 8a) and the very low Mg# of the chromites in sample 16-05 (Fig. 8b) are probably also the result of subsolidus, metamorphic re-equilibration via Mg–Ni and Mg–Fe exchange between co-existing minerals. A similar range of Mg# and Cr# in chromites were reported by Rollinson (2007) for ultramafic rocks from the Isua supracrustal belt. This is also observed in spinels within serpentinites from the Mesoarchean Tartoq Group in SW Greenland, which were overprinted to form high Cr# and Fe# during metamorphism associated with subduction zone accretion (Kisters et al., 2012; Szilas et al., 2013b, 2014b). This array is typical for amphibolite facies metamorphic disturbance of chromite (Evans and Frost, 1974; O'Hanley, 1996; Barnes and Roeder, 2001; Säntti et al., 2006; Bazylev et al., 2013) and is also consistent with the observation that Cr# and TiO<sub>2</sub> correlates positively (Fig. B3). This suggests residual enrichment during metamorphic reactions that would produce Al-bearing chlorite and/or amphiboles. If we use  $Fe^{3+}/Fe^{2+} < 10$ , as an indicator of the primary chromite grains, then the Cr# range becomes very tight at around 74 and the chromites from the ultramafic Isua rocks fall in the field of layered igneous complexes (cumulates). The fractional crystallisation trends that are observed from the major elements (Fig. 5) in combination with the fractionated PGE patterns (Fig. 7), suggest a cumulate origin for the ultramafic rocks, which these mineral compositions also support.

### 6.5. Petrogenetic implications

As we alluded to above, our data likely represent tholeiitic basalts, boninitic lavas, and their derivative ultramafic cumulates. To further test this hypothesis, we have calculated the liquid evolution by fractional crystallisation of primitive volcanic rocks from each of the two distinct magmatic trends in the Isua supracrustal belt using the MELTS software (Ghiorso and Sack, 1995; Asimow and Ghiorso, 1998). This allows us to compare the theoretical liquid evolution, as well as the corresponding cumulates, with the observed rocks at Isua. We assumed oxygen fugacity was buffered at QFM, that crystallisation occurred at 2 kbar and that initial water contents in the primitive magmas were 2 wt.%. We used sample 879320 from this study to model the boninitic trend and the median value of six tholeiitic basalt samples from Jenner et al. (2009) for the basaltic trend.

In Fig. 10, we show these two models for fractional crystallisation of olivine and spinel in comparison to the data from the Isua supracrustal belt. The calculated liquids generally follow the observed trends for the mafic Isua rocks. It is uncertain if plagioclase saturation was reached during the magmatic evolution of the observed mafic compositions, because this would result in abrupt changes in the CaO and Al<sub>2</sub>O<sub>3</sub> trends for the liquids. Likewise, orthopyroxene fractionation would be expected to result in elevated NiO in the liquids, rather than the observed, decreasing abundances with decreasing MgO. The discrepancy that we see for a few samples in terms of Cr and Ni, could possibly be explained by chromite and sulfide mineral precipitation, respectively. Polat and Hofmann (2003) also concluded that the geochemical variations in the volcanic suite of the Isua supracrustal belt were mainly controlled by olivine fractionation.

Nevertheless, though the model successfully reproduces the main features of chemical variation in the mafic rocks, interpreted as lava compositions, the corresponding dunite cumulates are different from the observed ultramafic rock compositions, which contain abundant normative orthopyroxene ± plagioclase in addition to olivine and

spinel. Thus, we infer that the cumulates record late crystallisation of plagioclase ± orthopyroxene and Fe–Ti oxides, with corresponding liquid compositions that were more evolved than the mafic rocks plotted in Fig. 10. Perhaps these evolved liquids were not preserved in the rock record, or perhaps such evolved compositions have gone unnoticed among the large suite of intermediate composition orthogneisses in the Isua region. From the modelling, accumulation of up to 32% plagioclase in addition to olivine and spinel could explain the observed range of compositions in the ultramafic rocks at Isua. Thus, crystallisation of this suite of cumulate minerals would shift the theoretical bulk cumulate compositions towards the volcanic trends for elements like Ca, Al and Mg. It is unlikely that orthopyroxene-saturation was reached, because this would result in norite cumulates, which have not been observed in the Isua volcanic sequence. Nevertheless, the presence of orthopyroxene is suggested by the slightly higher SiO<sub>2</sub> in the ultramafic rocks than in the predicted troctolite cumulate, and this is also hinted by the large amounts of normative orthopyroxene in these rocks. However, it is not possible to exclude that there could have been at least some degree of early silicification of the ultramafic rocks, which could have resulted in increased normative orthopyroxene relative to the modelled cumulate assemblage. Alternatively, interaction between the cumulates and the evolving liquids could also explain the apparent orthopyroxene contents (Fig. B1). Mixing between the evolving siliceous liquids and the dunite cumulates would be capable of producing abundant normative orthopyroxene in the ultramafic rocks, in addition to the observed geochemical trends (Fig. 5). Potential cumulate-liquid mixing could also explain the elevated incompatible trace element concentrations of the ultramafic rocks at Isua, which are nearly parallel with the volcanic rocks (Fig. 6). Indeed, binary mixing between depleted cumulates and evolved liquids of the two contrasting volcanic series would account for all of the linear trends that we observe in Fig. 10. Trapped inter-cumulus liquid would also be able to overprint the incompatible trace element inventory of the dunite cumulates, but this would not account for the high Al<sub>2</sub>O<sub>3</sub> contents of the cumulates relative to the liquids (Fig. 10). Reaction or impregnation by migrating liquids passing through the cumulate pile or perhaps in a magma conduit (feeder-pipe) remains a more realistic possibility for the elevated SiO<sub>2</sub> and incompatible trace element abundances relative to the modelled cumulates. However, based on our bulk-rock data alone, we cannot discriminate between these different types of potential cumulate-liquid interactions. Finally, as mentioned in Section 2, the ultramafic rocks can display uninterrupted transitions into gabbros in some areas of the Isua supracrustal belt (Nutman et al., 1996), which strongly supports the interpretation that these rocks are indeed cumulates formed by fractional crystallisation processes and are co-genetic with the associated mafic and boninitic volcanic rocks, regardless of the details of the cumulate-liquid interaction. As for the formation mechanism of these ultramafic cumulates we prefer a dynamic model in which melts and cumulates interacted during the eruption and fractional crystallisation, rather than a model with emplacement of a crystal mush (see Polat et al., 2012). We find the latter situation unlikely due to the fact that a cumulate mush becomes virtually rigid after about 40% crystallisation. It would also not account for the relatively large degrees of melt-cumulate mixing and more importantly, as stated above, the field observation of gabbros being in direct contact with some of the ultramafic rocks, suggests a tight association by in situ fractional crystallisation processes.

In summary, the data presented in this study are not consistent with the interpretation that the ultramafic rocks in the Isua supracrustal belt could represent mantle residues, as otherwise proposed by Friend and Nutman (2010, 2011). Instead the protoliths of these ultramafic rocks were likely olivine + spinel + plagioclase ± orthopyroxene cumulates derived from mafic magmas, as also suggested by previous workers (Dymek et al., 1988a, 1988b; Frei and Jensen, 2003; Rollinson, 2007; Hoffmann et al., 2011). The geochemical trends observed in these ultramafic rocks reflect variation in the cumulus mineralogy in combination

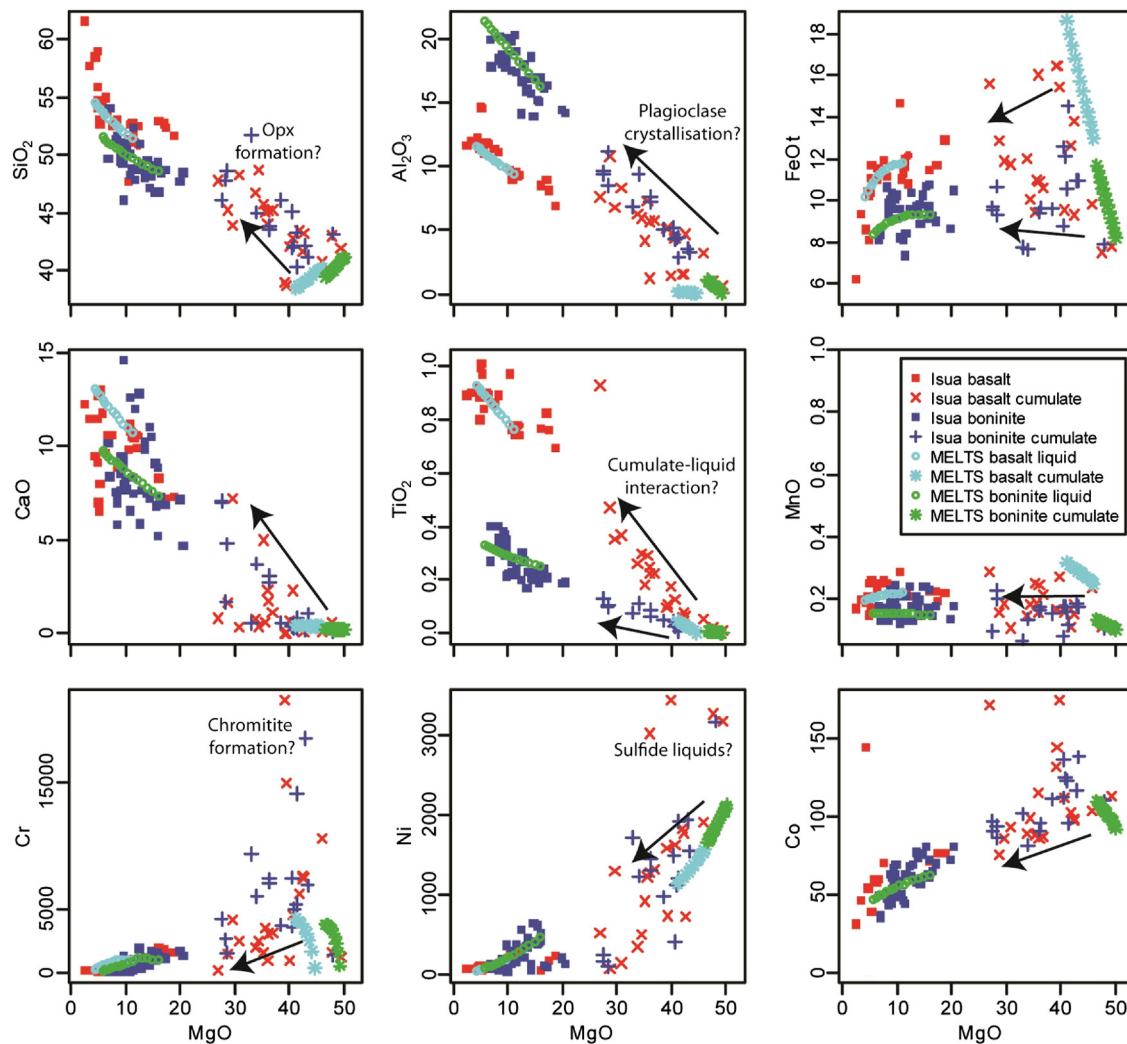


**Fig. 10.** Isua basalt and boninite data from this study, Polat et al. (2002, 2003) and Jenner et al. (2009) plotted together with MELTS calculations of the liquid evolution and the corresponding bulk cumulates during fractional crystallisation of olivine and spinel. Accumulation of plagioclase  $\pm$  orthopyroxene in combination with cumulate–liquid interaction, can account for the geochemical variation that is observed in the two distinct ultramafic rock trends of the Isua supracrustal belt. See Section 6.5 for a detailed discussion of these geochemical trends. NB. cobalt was not analysed in the basalts and therefore not modelled.

with variable degrees of cumulate–liquid interaction, such as by mixing, trapped inter-cumulus liquid, or melt impregnation/reaction (Fig. 10).

Our re-interpretation of the Isua dunites as being cumulates rather than mantle residues could lead some researchers to conclude that the rock assemblage of the Isua supracrustal belt is inconsistent with it representing an arc-related ophiolite, as otherwise proposed by previous workers (e.g., Furnes et al., 2007a,b; Dilek and Polat, 2008; Friend and Nutman, 2010; Nutman et al., 2013). However, that is not necessarily true given recent developments and the re-classification of ophiolites and Precambrian supracrustal belts (e.g., Dilek, 2003; Dilek and Furnes, 2011; Kusky et al., 2011; Dilek and Furnes, 2014; Furnes et al., 2014a). Of particular importance is the recognition that ophiolites do not always contain a mantle portion and many in fact only preserve the lower dunitic cumulates (e.g., Furnes et al., 1988, 1992). Equally important is the recognition that a sheeted dyke complex is not necessarily present in ophiolites (Robinson et al., 2008). In a recent compilation by Furnes et al. (2014b), which investigated 118 Phanerozoic ophiolites of which 75% are subduction-related, the occurrence of a sheeted dike complex was only reported in 47% of them. On a related note it is worth mentioning that Turner et al. (2014) recently presented chemostratigraphic similarities between the Eoarchaean Nuvvuagittuq greenstone sequence in Canada, and that of the Izu–Bonin–Mariana

forearc. A similar model could potentially be applicable to the Isua supracrustal belt.

Given the island arc tholeiitic and boninitic affinities of the volcanic rocks of the Isua supracrustal belt, the presence of lower crustal cumulates and the general tectonic evolution, this rock assemblage does indeed appear to be consistent with the interpretation that it formed as an Eoarchaean arc-related ophiolite.

## 7. Conclusions

Several lines of evidence lead us to conclude that the protoliths of the ultramafic rocks in the Isua supracrustal belt cannot represent mantle residues, but were rather igneous cumulates, which formed by accumulation of olivine + spinel + plagioclase  $\pm$  orthopyroxene in addition to interaction with the evolving liquids:

- Olivine and spinel compositions overlap with igneous compositions known from basalts and boninites, as well as from metamorphic rocks. The few spinel grains that could potentially reflect primary igneous compositions have Cr# of around 73 and most have Mg# of about 23, which are not typical of mantle residues.
- Bulk-rock geochemical compositions are unlike those of mantle residues. In particular, the relatively high FeOt contents (up to 16 wt.%),

Al<sub>2</sub>O<sub>3</sub> contents (up to 11 wt.%), elevated incompatible trace element concentrations, and the trends towards the two distinct local volcanic series are consistent with a cumulate origin for the ultramafic rocks.

- Platinum-group element patterns are fractionated with low Os and Ir abundances (~0.001× chondrite), whereas mantle residues typically have flat patterns and higher Os and Ir abundances (~0.01× chondrite). The PGE abundances of the Isua rocks may imply that their Eoarchaean mantle sources had already equilibrated with the PGE-contribution from the “late veneer”.
- Modelling of compositional trends for liquids and corresponding cumulates of the Isua basalts and boninitic series agrees reasonably well with the observed geochemical data. The most refractory ultramafic samples overlap with predicted olivine + spinel cumulate compositions. Less refractory ultramafic rocks, with abundant normative orthopyroxene ± plagioclase overlap with calculated olivine + spinel in addition to plagioclase ± orthopyroxene bulk cumulates and are therefore interpreted to have formed via continued crystallisation of more evolved liquid compositions, that are either missing from the rock record or present, but not yet identified. Alternatively, the normative orthopyroxene is either the result of early addition of SiO<sub>2</sub> by silicification or the result of interaction between the evolving liquids and dunite cumulates. Regardless of the exact details, variable proportions of typically crystallising minerals in combination with cumulate–liquid interaction can account for the full range of geochemical variation that is observed for the ultramafic rocks in the Isua supracrustal belt.

Supplementary data to this article can be found online at <http://dx.doi.org/10.1016/j.gr.2014.07.010>.

## Acknowledgements

We are grateful for samples provided by Emily C. Pope, Dennis K. Bird, and J. Elis Hoffmann, which made this study possible. We also thank Ole Christiansen of NunaMinerals A/S for giving us access to drill core material. We appreciate comments on an early version of the manuscript by J. Elis Hoffmann, Jakob K. Keiding, Lotte M. Larsen, and Stephen Moorbath, which improved this work. We thank Harald Furnes and one anonymous reviewer for constructive comments, which placed our study into a proper context. Tim Kusky is thanked for the editorial handling of the manuscript. K. Szilas was supported by grant no. 12-125873 from The Danish Council for Independent Research, Natural Sciences (FNU). The Nordic Center for Earth Evolution is supported by The Danish National Research Foundation. LDEO contribution #7819. This study is a contribution to IGCP-SIDA project 599.

## References

- Alard, O., Griffin, W.L., Lorand, J.P., Jackson, S.E., O'Reilly, S.Y., 2000. Non-chondritic distribution of highly siderophile elements in mantle sulfides. *Nature* 407, 891–894.
- Allaart, J.H., 1976. The pre-3760 m.y. old supracrustal rocks of the Isua area, central West Greenland, and the associated occurrence of quartz-banded ironstone. In: Windley, B.F. (Ed.), *The Early History of the Earth*. Wiley, London, pp. 177–189.
- Appel, P.W.U., Fedo, C.M., Moorbath, S., Myers, J.S., 1998. Recognizable primary volcanic and sedimentary features in a low strain domain of the highly deformed, oldest known (~3.7–3.8 Gyr) Greenstone Belt, Isua, West Greenland. *Terra Nova* 10, 57–62.
- Appel, P.W.U., Polat, A., Frei, R., 2009. Dactylic ocelli in mafic lavas, 3.8–3.7 Ga Isua greenstone belt, West Greenland: geochemical evidence for partial melting of oceanic crust and magma mixing. *Chemical Geology* 258, 105–124.
- Arndt, N., Leshar, M.C., Barnes, S.J., 2008. *Komatiite*. Cambridge University Press, (467 pp.).
- Asimow, P.D., Ghiorso, M.S., 1998. Algorithmic modifications extending MELTS to calculate subsolidus phase relations. *American Mineralogist* 83, 1127–1132.
- Ballhaus, C., Bockrath, C., Wohlgemuth-Ueberwasser, C., Laurenz, V., Berndt, J., 2006. Fractionation of noble metals by physical processes. *Contributions to Mineralogy and Petrology* 152, 667–684.
- Barnes, S.J., Picard, C.P., 1993. The behaviour of platinum-group elements during partial melting, crystal fractionation, and sulphide segregation: an example from the Cape Smith Fold Belt, northern Quebec. *Geochimica et Cosmochimica Acta* 57, 79–87.
- Barnes, S.J., Roeder, P.L., 2001. The range of spinel compositions in terrestrial mafic and ultramafic rocks. *Journal of Petrology* 42, 2279–2302.
- Barnes, S.-J., Naldrett, A.J., Gorton, M.P., 1985. The origin of fractionation of platinum-group elements in terrestrial magmas. *Chemical Geology* 53, 303–323.
- Bazylev, B.A., Ledneva, G.V., Kononkova, N.N., Ishiwatari, A., 2013. High-pressure ultramafics in the lower crustal rocks of Pekul'ny Complex, Central Chukchi Peninsula. 1. Petrography and mineralogy. *Petrology* 21, 221–248.
- Becker, H., Horan, M.F., Walker, R.J., Gao, S., Lorand, J.P., Rudnick, R.L., 2006. Highly siderophile element composition of the Earth's primitive upper mantle: constraints from new data on peridotite massifs and xenoliths. *Geochimica et Cosmochimica Acta* 70, 4528–4550.
- Bédard, J.H., Lauziere, K., Tremblay, A., Sangster, A., 1998. Evidence for forearc seafloor-spreading from Betts cove ophiolite, Newfoundland: oceanic crust of boninitic affinity. *Tectonophysics* 284, 233–245.
- Bennett, V.C., Nutman, A.P., McCulloch, M.T., 1993. Nd isotopic evidence for transient, highly depleted mantle reservoirs in the early history of the Earth. *Earth and Planetary Science Letters* 119, 299–317.
- Bennett, V.C., Nutman, A.P., Esat, T.M., 2002. Constraints on mantle evolution from 187Os/188Os isotopic compositions from Archaean ultramafic rocks from southern west Greenland (3.8 Ga) and western Australia (3.46 Ga). *Geochimica et Cosmochimica Acta* 66, 2615–2630.
- Bennett, V.C., Brandon, A., Nutman, A.P., 2007. Coupled 142Nd–143Nd isotopic evidence for Hadean mantle dynamics. *Science* 318, 1907–1910.
- Bernstein, S., Szilas, K., Kelemen, P.B., 2013. Highly depleted cratonic mantle in West Greenland extending into diamond stability field in the Proterozoic. *Lithos* 168, 160–172.
- Bézos, A., Lorand, J.-P., Humler, E., Gros, M., 2005. Platinum-group element systematics in mid-ocean ridge basaltic glasses from the Pacific, Atlantic and Indian Oceans. *Geochimica et Cosmochimica Acta* 69, 2613–2627.
- Blichert-Toft, J., Frei, R., 2001. Complex Sm–Nd and Lu–Hf isotope systematics in metamorphic garnets from the Isua supracrustal belt, West Greenland. *Geochimica et Cosmochimica Acta* 65, 3177–3189.
- Boak, J.L., Dymek, R.F., 1982. Metamorphism of the ca. 3800 Ma supracrustal rocks at Isua, West Greenland: implications for early Archaean crustal evolution. *Earth and Planetary Science Letters* 59, 155–176.
- Bolhar, R., Kamber, B.S., Moorbath, S., Fedo, C.M., Whitehouse, M.J., 2004. Characterisation of early Archaean chemical sediments by trace element signatures. *Earth and Planetary Science Letters* 222, 43–60.
- Boyett, M., Blichert-Toft, J., Rosing, M., Storey, M., Télouk, P., Albarède, F., 2003. 142Nd evidence for early Earth differentiation. *Earth and Planetary Science Letters* 214, 427–442.
- Caro, G., Bourdon, B., Birk, J.-L., Moorbath, S., 2003. 146Sm–142Nd evidence from Isua metasediments for early differentiation of Earth's mantle. *Nature* 423, 428–432.
- Coggon, J.A., Luguet, A., Nowell, G.M., Appel, P.W., 2013. Hadean mantle melting recorded by southwest Greenland chromitite 186Os signatures. *Nature Geoscience* 6, 871–874.
- Crocket, J.H., 2000. PGE in fresh basalt, hydrothermal alteration products, and volcanic incrustations of Kilauea volcano, Hawaii. *Geochimica et Cosmochimica Acta* 64, 1791–1807.
- Crowley, J.L., 2003. U–Pb geochronology of 3810–3630 Ma granitoid rocks south of the Isua greenstone belt, southern West Greenland. *Precambrian Research* 126, 235–257.
- Dale, C.W., Burton, K.W., Greenwood, R.C., Gannoun, A., Wade, J., Wood, B.J., Pearson, D.G., 2012. Late accretion on the earliest planetesimals revealed by the highly siderophile elements. *Science* 336, 72–75.
- Day, J.M., Walker, R.J., Qin, L., Rumble III, D., 2012. Late accretion as a natural consequence of planetary growth. *Nature Geoscience* 5, 614–617.
- De Hoog, J.C., Janak, M., Vrabec, M., Hattori, K.H., 2011. Ultramafic cumulates of oceanic affinity in an intracontinental subduction zone: ultrahigh-pressure garnet peridotites from Pohorje (Eastern Alps, Slovenia). In: Dobrzynetska, L., Faryad, S.W., Wallis, S., Cuthbert, S. (Eds.), *Ultrahigh-Pressure Metamorphism: 25 Years After The Discovery Of Coesite And Diamond*. Elsevier, London, pp. 399–439.
- Deschamps, F., Godard, M., Guillot, S., Hattori, K., 2013. Geochemistry of subduction zone serpentinites: a review. *Lithos* 178, 96–127.
- Dick, H.J., Bullen, T., 1984. Chromian spinel as a petrogenetic indicator in abyssal and alpine-type peridotites and spatially associated lavas. *Contributions to Mineralogy and Petrology* 86, 54–76.
- Dilek, Y., 2003. Ophiolite concept and its evolution. In: Dilek, Y., Newcomb, S. (Eds.), *Ophiolite Concept and the Evolution of Geological Thought*. Geological Society of America, Special Paper. 373, pp. 1–16.
- Dilek, Y., Furnes, H., 2011. Ophiolite genesis and global tectonics: geochemical and tectonic fingerprinting of ancient oceanic lithosphere. *Geological Society of America Bulletin* 123, 387–411.
- Dilek, Y., Furnes, H., 2014. Ophiolites and their origins. *Elements* 10, 93–100.
- Dilek, Y., Polat, A., 2008. Suprasubduction zone ophiolites and Archaean tectonics. *Geology* 36, 431–432.
- Dymek, R.F., Brothers, S.C., Schiffrins, C.M., 1988a. Petrogenesis of ultramafic metamorphic rocks from the 3800 Ma Isua supracrustal belt, West Greenland. *Journal of Petrology* 29, 1353–1397.
- Dymek, R.F., Brothers, S.C., Schiffrins, C.M., 1988b. Titanian chondrodite- and titanian clinohumite-bearing metadunite from the 3800 Ma Isua supracrustal belt, West Greenland: chemistry, petrology and origin. *American Mineralogist* 73, 547–558.
- Dziggel, A., Diener, J.F.A., Kolb, J., Kokfelt, T.F., 2014. Metamorphic record of accretionary processes during the Neoproterozoic: the Nuuk region, southern West Greenland. *Precambrian Research* 242, 22–38.
- Escayola, M., Garuti, G., Zaccarini, F., Proenza, J.A., Bédard, J.H., Van Staal, C., 2011. Chromitite and platinum-group-element mineralization at middle Arm Brook, central Advocate ophiolite complex, Baie Verte peninsula, Newfoundland, Canada. *The Canadian Mineralogist* 49, 1523–1547.

- Evans, B.W., Frost, B.R., 1974. Chrome-spinel in progressive metamorphism – a preliminary analysis. *Geochimica et Cosmochimica Acta* 39, 959–972.
- Fiorentini, M.L., Barnes, S.J., Maier, W.D., Burnham, O.M., Heggie, G., 2011. Global variability in the platinum-group element contents of komatiites. *Journal of Petrology* 52, 83–112.
- Fisher-Gödde, M., Becker, H., Wombacher, F., 2010. Rhodium, gold and other highly siderophile element abundances in chondritic meteorites. *Geochimica et Cosmochimica Acta* 74, 356–379.
- Frei, R., Jensen, B.K., 2003. Re–Os, Sm–Nd isotope- and REE systematics on ultramafic rocks and pillow basalts from the Earth's oldest oceanic crustal fragments (Isua supracrustal belt and Ujaragssuit nunat area, W Greenland). *Chemical Geology* 196, 163–191.
- Frei, R., Rosing, M.T., 2001. The least radiogenic terrestrial leads; implications for the early Archean crustal evolution and hydrothermal–metasomatic processes in the Isua Supracrustal Belt (West Greenland). *Chemical Geology* 181, 47–66.
- Frei, R., Bridgwater, D., Rosing, M., Stecher, O., 1999. Controversial Pb–Pb and Sm–Nd isotope results in the early Archean Isua (West Greenland) oxide iron formation: preservation of primary signatures versus secondary disturbances. *Geochimica et Cosmochimica Acta* 63, 473–488.
- Frei, R., Rosing, M.T., Waight, T.E., Ulfbeck, D.G., 2002. Hydrothermal–metasomatic and tectono–metamorphic processes in the Isua supracrustal belt (West Greenland): a multi-isotopic investigation of their effects on the Earth's oldest oceanic crustal sequence. *Geochimica et Cosmochimica Acta* 66, 467–486.
- Frei, R., Polat, A., Meibom, A., 2004. The Hadean upper mantle conundrum: evidence for source depletion and enrichment from Sm–Nd, Re–Os, and Pb isotopic compositions in 3.71 Gy boninite-like metabasalts from the Isua Supracrustal Belt, Greenland. *Geochimica et Cosmochimica Acta* 68, 1645–1660.
- Friend, C.R., Nutman, A.P., 2005a. New pieces to the Archaean terrane jigsaw puzzle in the Nuuk region, southern West Greenland: steps in transforming a simple insight into a complex regional tectonothermal model. *Journal of the Geological Society* 162, 147–162.
- Friend, C.R.L., Nutman, A.P., 2005b. Complex 3670–3500 Ma orogenic episodes superimposed on juvenile crust accreted between 3850–3690 Ma, Itsaq Gneiss Complex, southern West Greenland. *Journal of Geology* 113, 375–398.
- Friend, C.R.L., Nutman, A.P., 2010. Eoarchean ophiolites? New evidence for the debate on the Isua supracrustal belt, southern West Greenland. *American Journal of Science* 310, 826–861.
- Friend, C.R.L., Nutman, A.P., 2011. Dunites from Isua, Greenland: a ca. 3720 Ma window into subcrustal metasomatism of depleted mantle. *Geology* 39, 663–666.
- Friend, C.R.L., Nutman, A.P., McGregor, V.R., 1988. Late Archaean terrane accretion in the Godthåb region, southern West Greenland. *Nature* 335, 535–538.
- Friend, C.R.L., Bennett, V.C., Nutman, A.P., 2002. Abyssal peridotites >3,800 Ma from southern West Greenland: field relationships, petrography, geochronology, whole-rock and mineral chemistry of dunite and harzburgite inclusions in the Itsaq Gneiss Complex. *Contributions to Mineralogy and Petrology* 143, 71–92.
- Furnes, H., Pedersen, R.B., Stillman, C.J., 1988. The Leka Ophiolite Complex, central Norwegian Caledonides: field characteristics and geotectonic significance. *Journal of the Geological Society, London* 145, 401–412.
- Furnes, H., Pedersen, R.B., Hertogen, J., Albrektsen, B.A., 1992. Magma development of the Leka Ophiolite Complex, central Norwegian Caledonides. *Lithos* 27, 259–277.
- Furnes, H., de Wit, M., Staudigel, H., Rosing, M., Muehlenbachs, K., 2007a. A vestige of Earth's oldest ophiolite. *Science* 315, 1704–1707.
- Furnes, H., de Wit, M., Staudigel, H., Rosing, M., Muehlenbachs, K., 2007b. Response to comments on "A Vestige of Earth's Oldest Ophiolite". *Science* 318, 746e.
- Furnes, H., Rosing, M., Dilek, Y., De Wit, M., 2009. Isua supracrustal belt (Greenland) – A vestige of a 3.8 Ga suprasubduction zone ophiolite, and the implications for Archean geology. *Lithos* 113, 115–132.
- Furnes, H., de Wit, M., Dilek, Y., 2014a. Precambrian greenstone belts host different ophiolite types. In: Dilek, Y., Furnes, H. (Eds.), *Evolution of Archean Crust and Early Life*. Springer, Netherlands, pp. 1–22.
- Furnes, H., de Wit, M., Dilek, Y., 2014b. Four billion years of ophiolites reveal secular trends in oceanic crust formation. *Geoscience Frontiers* 5, 571–603.
- Garde, A.A., 2007. A mid-Archaean island arc complex in the eastern Akia terrane, Godthåbsfjord, southern West Greenland. *Journal of the Geological Society* 164, 565–579.
- Garrido, C.J., Bodinier, J.-L., Dhuime, B., Bosch, D., Chanefo, I., Bruguier, O., Hussain, S.S., Dawood, H., Burg, J.-P., 2007. Origin of the island arc Moho transition zone via melt–rock reaction and its implication for intracrustal differentiation of island arcs: evidence from the Jijal complex (Kohistan complex, northern Pakistan). *Geology* 35, 683–686.
- Ghiorsio, M.S., Sack, R.O., 1995. Chemical mass transfer in magmatic processes IV. A revised and internally consistent thermodynamic model for the interpolation and extrapolation of liquid–solid equilibria in magmatic systems at elevated temperatures and pressures. *Contributions to Mineralogy and Petrology* 119, 197–212.
- Grant, J.A., 1986. The isocon diagram – a simple solution to Gresens' equation for metasomatic alteration. *Economic Geology* 81, 1976–1982.
- Gresens, R.L., 1967. Composition–volume relationships of metasomatism. *Chemical Geology* 2, 47–55.
- Guillot, S., Hattori, K.H., De Sigoyer, J., 2000. Mantle wedge serpentinisation and exhumation of eclogites: insights from eastern Ladakh, northwest Himalaya. *Geology* 28, 199–202.
- Hamilton, W.B., 2007. Comment on "A vestige of Earth's oldest ophiolite". *Science* 318, 746d.
- Hanghøj, K., Kelemen, P.B., Hassler, D., Godard, M., 2010. Composition and genesis of depleted mantle peridotites from the Wadi Tayin Massif, Oman Ophiolite; major and trace element geochemistry, and Os isotope and PGE systematics. *Journal of Petrology* 51, 201–227.
- Hannmer, S., Greene, D.C., 2002. A modern structural regime in the Paleoproterozoic (~3.64 Ga); Isua Greenstone Belt, southern West Greenland. *Tectonophysics* 346, 201–222.
- Hattori, K., Hart, S.R., 1997. PGE and Os isotopic signatures for ultramafic rocks from the base of the Talkeetna island arc, Alaska. *Eos* 78, 339.
- Hattori, K., Shirahase, T., 1997. Platinum group elements and osmium isotope signatures of the Kohistan island arc sequence, Himalaya–Karakoram area. *Eos* 78, 829.
- Hattori, K., Wallis, S., Enami, M., Mizukami, T., 2010. Subduction of mantle wedge peridotites: evidence from the Hihashi-akaishi ultramafic body in the Sanbagawa metamorphic belt. *Island Arc* 19, 192–207.
- Hoffmann, J.E., Münker, C., Polat, A., König, S., Mezger, K., Rosing, M.T., 2010. Highly depleted Hadean mantle reservoirs in the sources of early Archean arc-like rocks, Isua supracrustal belt, southern West Greenland. *Geochimica et Cosmochimica Acta* 74, 7236–7260.
- Hoffmann, J.E., Münker, C., Polat, A., Rosing, M.T., Schulz, T., 2011. The origin of decoupled Hf–Nd isotope compositions in Eoarchean rocks from southern West Greenland. *Geochimica et Cosmochimica Acta* 75, 6610–6628.
- Hoffmann, J., Nagel, T.J., Münker, C., Næraa, T., Rosing, M.T., 2014. Constraining the process of Eoarchean TTG formation in the Itsaq Gneiss Complex, southern West Greenland. *Earth and Planetary Science Letters* 388, 374–386.
- Huang, H., Polat, A., Fryer, B.J., 2013. Origin of Archean tonalite–trondhjemite–granodiorite (TTG) suites and granites in the Fiskensæset region, southern West Greenland: implications for continental growth. *Gondwana Research* 23, 452–470.
- Huang, H., Fryer, B.J., Polat, A., Pan, Y., 2014. Amphibole, plagioclase and clinopyroxene geochemistry of the Archean Fiskensæset Complex at Majorqap qáva, southwestern Greenland: implications for Archean petrogenetic and geodynamic processes. *Precambrian Research* 247, 64–91.
- Iizuka, T., Nakai, S.I., Sahoo, Y.V., Takamasa, A., Hirata, T., Maruyama, S., 2010. The tungsten isotopic composition of Eoarchean rocks: implications for early silicate differentiation and core–mantle interaction on Earth. *Earth and Planetary Science Letters* 291, 189–200.
- Jagoutz, O., Schmidt, M.W., 2013. The composition of the foundered complement to the continental crust and a re-evaluation of fluxes in arcs. *Earth and Planetary Science Letters* 371–372, 177–190.
- Janosek, V., Farrow, C.M., Erban, V., 2006. Interpretation of whole-rock geochemical data in igneous geochemistry: introducing Geochemical Data Tool (GCDkit). *Journal of Petrology* 47, 1255–1259.
- Jenner, F.E., Bennett, V.C., Nutman, A.P., Friend, C.R.L., Norman, M.D., Yaxley, G., 2009. Evidence for subduction at 3.8 Ga: geochemistry of arclike metabasalts from the southern edge of the Isua Supracrustal Belt. *Chemical Geology* 261, 82–99.
- Jensen, B.K., 2002. Os and Pb isotopic study of ultramafics of the Isua supracrustal belt West Greenland. Unpublished M.Sc. thesis, University of Copenhagen, 133 pp.
- Johnson, K.E., Brady, J.B., MacFarlane, W.A., Thomas, R.B., Poulsen, C.J., Sincock, M.J., 2004. Precambrian meta-ultramafic rocks from the Tobacco Root Mountains, Montana. *Geological Society of America Special Papers* 377, 71–88.
- Kamber, B.S., Whitehouse, M.J., Bolhar, R., Moorbath, S., 2005. Volcanic resurfacing and the early terrestrial crust: zircon U–Pb and REE constraints from the Isua Greenstone Belt, southern West Greenland. *Earth and Planetary Science Letters* 240, 276–290.
- Kelemen, P.B., Dick, H.J.B., Quick, J.E., 1992. Formation of harzburgite by pervasive melt/rock reaction in the upper mantle. *Nature* 358, 635–641.
- Kelemen, P.B., Hart, S.R., Bernstein, S., 1998. Silica enrichment in the continental upper mantle via melt/rock reaction. *Earth and Planetary Science Letters* 164, 387–406.
- Kelemen, P.B., Hanghøj, K., Greene, A., 2003. One view of the geochemistry of subduction-related magmatic arcs, with an emphasis on primitive andesite and lower crust. In: Rudnick, R.L. (Ed.), *The Crust: The Crust: Holland, H.D., Turekian, K.K. (Eds.), Treatise on Geochemistry*. vol. 3. Elsevier–Pergamon, Oxford, UK, pp. 593–659.
- Kerrich, R., Wyman, D., Fan, J., Bleeker, W., 1998. Boninite series: low Ti–tholeiite associations from the 2.7 Ga Abitibi greenstone belt. *Earth and Planetary Science Letters* 164, 303–316.
- Keto, L., 1970. Isua, a major iron ore discovery in Greenland. *Kryolitselskabet Øresund A/S. Abstract Nordic Winter Meeting, Copenhagen*.
- Keto, L., Kurki, J., 1967. Report on the exploration activity at Isua 1967. *Kryolitselskabet Øresund A/S prospecting report lodged as report 20024 at the Geological Survey of Denmark and Greenland*.
- Kisters, A.F., van Hinsberg, V.J., Szilas, K., 2012. Geology of an Archaean accretionary complex—the structural record of burial and return flow in the Tartuq Group of South West Greenland. *Precambrian Research* 220, 107–122.
- Kodolányi, J., Pettek, T., Spandler, C., Kamber, B.S., Gméling, K., 2012. Geochemistry of ocean floor and fore-arc serpentinites: constraints on the ultramafic input to subduction zones. *Journal of Petrology* 53, 235–270.
- Komiya, T., Maruyama, S., Masuda, T., Nohda, S., Hayashi, M., Okamoto, K., 1999. Plate tectonics at 3.8–3.7 Ga: field evidence from the Isua accretionary complex, southern West Greenland. *Journal of Geology* 107, 515–554.
- Kurki, J., Keto, L., 1966. Report on geological investigations at Isua 1966. *Kryolitselskabet Øresund A/S prospecting report lodged as report 20219 at the Geological Survey of Denmark and Greenland*.
- Kusky, T.M., Wang, L., Dilek, Y., Robinson, P., Peng, S.B., Huang, X.Y., 2011. Application of the modern ophiolite concept with special reference to Precambrian ophiolites. *Science China–Earth Sciences* 54, 315–341.
- Liu, Y., Zong, K., Kelemen, P.B., Gao, S., 2008. Geochemistry and magmatic history of eclogites and ultramafic rocks from the Chinese continental scientific drill hole: subduction and ultrahigh-pressure metamorphism of lower crustal cumulates. *Chemical Geology* 247, 133–153.
- Locmelis, M., Pearson, N.J., Barnes, S.J., Fiorentini, M.L., 2011. Ruthenium in komatiitic chromite. *Geochimica et Cosmochimica Acta* 75, 3645–3661.

- Lorand, J.-P., 1989. Are spinel lherzolite xenoliths representative of the abundances of sulphur in the upper mantle? *Geochimica et Cosmochimica Acta* 54, 1487–1492.
- Lorand, J.-P., Alard, O., Godard, M., 2008. Platinum-group element signatures of the primitive mantle rejuvenated by melt–rock reactions: evidence from Sumail peridotites (Oman Ophiolite). *Terra Nova* 21, 35–40.
- Luguet, A., Shirey, S.B., Lorand, J.-P., Horan, M.F., Carlson, R.W., 2007. Residual platinum-group minerals from highly depleted harzburgites of the Lherz massif (France) and their role in HSE fractionation of the mantle. *Geochimica et Cosmochimica Acta* 71, 3082–3097.
- Marchesi, C., Garrido, C.J., Godard, M., Belley, F., Ferré, E., 2009. Migration and accumulation of ultra-depleted subduction-related melts in the Massif du Sud ophiolite (New Caledonia). *Chemical Geology* 266, 171–186.
- Marchesi, C., Garrido, C.J., Padrón-Navarra, J.A., Sánchez-Vizcaino, V.L., Gómez-Pugnaire, M.T., 2013a. Element mobility from seafloor serpentinisation to high-pressure dehydration of antigorite in subducted serpentinite: insights from the Cerro del Almirez ultramafic massif (southern Spain). *Lithos* 178, 128–142.
- Marchesi, C., Garrido, C.J., Harvey, J., González-Jiménez, J.M., Hidas, K., Lorand, J.P., Gervilla, F., 2013b. Platinum-group elements, S, Se and Cu in highly depleted abyssal peridotites from the Mid-Atlantic Ocean Ridge (ODP Hole 1274A): influence of hydrothermal and magmatic processes. *Contributions to Mineralogy and Petrology* 166, 1521–1538.
- Maruyama, S., Masuda, T., Nohda, S., Appel, P., Otofuji, Y., Miki, M., Shibata, T., Hagiya, H., 1992. The 3.9–3.8 Ga plate tectonics on the Earth: evidence from Isua, Greenland. Abstract presented at the Evolving Earth Symposium. Tokyo Institute of Technology, Okazaki, Japan.
- Momme, P., Tegner, C., Brooks, C.K., Keays, R.R., 2002. The behaviour of platinum-group elements in basalts from the East Greenland rift margin. *Contributions to Mineralogy and Petrology* 143, 133–153.
- Moorbath, S., O'Nions, R.K., Pankhurst, R.J., Gale, N.H., McGregor, V.R., 1972. Further rubidium–strontium age determinations on the very early Precambrian rocks of the Godthåb district: West Greenland. *Nature* 240, 78–82.
- Moorbath, S., O'Nions, R.K., Pankhurst, R.J., 1973. Early Archaean age for the Isua iron formation, West Greenland. *Nature* 245, 138–139.
- Moorbath, S., O'Nions, R.K., Pankhurst, R.J., 1975. The evolution of early Precambrian crustal rocks at Isua, West Greenland—geochemical and isotopic evidence. *Earth and Planetary Science Letters* 27, 229–239.
- Moorbath, S., Allaart, J.H., Bridgwater, D., McGregor, V.R., 1977. Rb–Sr ages of early Archaean supracrustal rocks and Amitsoq gneisses at Isua. *Nature* 270, 43–45.
- Moorbath, S., Whitehouse, M.J., Kamber, B.S., 1997. Extreme Nd-isotope heterogeneity in the early Archaean—fact or fiction? Case histories from northern Canada and West Greenland. *Chemical Geology* 135, 213–231.
- Myers, J.S., 2001. Protoliths of the 3.8–3.7 Ga Isua greenstone belt, West Greenland. *Precambrian Research* 105, 129–141.
- Næraa, T., Scherstén, A., Rosing, M.T., Kemp, A.I.S., Hoffmann, J.E., Kokfelt, T.F., Whitehouse, M.J., 2012. Hafnium isotope evidence for a transition in the dynamics of continental growth 3.2 Gyr ago. *Nature* 485, 627–630.
- Nagel, T.J., Hoffmann, J.E., Münker, C., 2012. Generation of Eoarchean tonalite–trondhjemite–granodiorite series from thickened mafic arc crust. *Geology* 40, 375–378.
- Nielsen, T.F.D., 1981. The ultramafic cumulates series, Gardiner Complex, East Greenland—Cumulates in a shallow level magma chamber of a nephelinitic volcano. *Contributions to Mineralogy and Petrology* 76, 60–72.
- Niu, Y., 2004. Bulk-rock major and trace element compositions of abyssal peridotites: implications for mantle melting, melt extraction and post-melting processes beneath mid-ocean ridges. *Journal of Petrology* 45, 2423–2458.
- Nutman, A.P., 1986. The geology of the Isukasia region, southern West Greenland. *Grønlands Geologiske Undersøgelse Bulletin* 154 (80 pp.).
- Nutman, A.P., Friend, C.R.L., 2007a. Comment on “A vestige of Earth's oldest ophiolite”. *Science* 318, 746c.
- Nutman, A.P., Friend, C.R., 2007b. Adjacent terranes with ca. 2715 and 2650 Ma high-pressure metamorphic assemblages in the Nuuk region of the North Atlantic Craton, southern West Greenland: complexities of Neoarchaean collisional orogeny. *Precambrian Research* 155, 159–203.
- Nutman, A.P., Friend, C.R.L., 2009. New 1:20,000 scale geological maps, synthesis and history of investigation of the Isua supracrustal belt and adjacent orthogneisses, southern West Greenland: a glimpse of Eoarchaean crust formation and orogeny. *Precambrian Research* 172, 189–211.
- Nutman, A.P., McGregor, V.R., Friend, C.R.L., Bennett, V.C., Kinny, P.D., 1996. The Itsaq Gneiss Complex of southern West Greenland: the world's most extensive record of early crustal evolution (3900–3600 Ma). *Precambrian Research* 78, 1–39.
- Nutman, A.P., Bennett, V.C., Friend, C.R.L., Rosing, M.T., 1997. ~3710 and ≥3790 Ma volcanic sequences in the Isua (Greenland) supracrustal belt: structural and Nd isotope implications. *Chemical Geology* 141, 271–287.
- Nutman, A.P., Bennett, V.C., Friend, C.R.L., Norman, M.D., 1999. Meta-igneous (nongneissic) tonalites and quartz–diorites from an extensive ca. 3800 Ma terrain south of the Isua supracrustal belt, southern West Greenland: constraints on early crust formation. *Contributions to Mineralogy and Petrology* 137, 364–388.
- Nutman, A.P., Friend, C.R.L., Bennett, V.C., 2002. Evidence for 3650–3600 Ma assembly of the northern end of the Itsaq Gneiss Complex, Greenland: implication for early Archaean tectonics. *Tectonics* 21 (article 5).
- Nutman, A.P., Friend, C.R.L., Barker, S.L.L., McGregor, V.R., 2004. Inventory and assessment of Palaeoarchaean gneiss terrains and detrital zircons in southern West Greenland. *Precambrian Research* 135, 281–314.
- Nutman, A.P., Friend, C.R.L., Horie, H., Hidaka, H., 2007. Construction of pre-3600 Ma crust at convergent plate boundaries, exemplified by the Itsaq Gneiss Complex of southern West Greenland. In: van Kranendonk, M.J., Smithies, R.H., Bennett, V.C. (Eds.), *Earth's Oldest Rocks*. Elsevier, pp. 187–218.
- Nutman, A.P., Bennett, V.C., Friend, C.R.L., Jenner, F., Wan, Y., Liu, D.-Y., 2009a. Episodic Eoarchaean crustal accretion (3.87 to 3.66 Ga) in West Greenland (Itsaq Gneiss Complex) and in northeastern China. In: Cawood, P.A., Kröner, A. (Eds.), *Earth Accretionary Systems in Space and Time*. Special Publication of the Geological Society, 318, pp. 127–154.
- Nutman, A.P., Friend, C.R.L., Paxton, S., 2009b. Detrital zircon sedimentary provenance ages for the Eoarchaean Isua supracrustal belt, southern West Greenland: juxtaposition of an imbricated ca. 3700 Ma juvenile arc assemblage against an older complex with 3920–3800 Ma components. *Precambrian Research* 172, 212–233.
- Nutman, A.P., Bennett, V.C., Friend, C.R., 2013. The emergence of the Eoarchaean protocrust: evolution of a c. 3700 Ma convergent plate boundary at Isua, southern West Greenland. Geological Society, London, Special Publications 389, SP389-5.
- O'Hanley, D.S., 1996. Serpentinites: Records of Tectonic and Petrological History. Oxford University Press, New York, (277 pp.).
- Ordóñez-Calderón, J.C., Polat, A., Fryer, B.J., Gagnon, J.E., Raith, J.G., Appel, P.W.U., 2008. Evidence for HFSE and REE mobility during calc–silicate metasomatism, Mesoarchean (~3075 Ma) Ivisartoq greenstone belt, southern West Greenland. *Precambrian Research* 161, 317–340.
- Palme, H., O'Neill, H.C., 2003. Compositional estimates of mantle composition. In: Carlson, R.W. (Ed.), *The Mantle and Core*: Holland, H.D., Turekian, K.K. (Eds.), *Treatise on Geochemistry*. vol. 2. Elsevier-Perigamon, Oxford, UK, pp. 1–38.
- Paulick, H., Bach, W., Godard, M., De Hoog, J.C.M., Suhr, G., Harvey, J., 2006. Geochemistry of abyssal peridotites (Mid-Atlantic Ridge, 15°20'N, ODP Leg 209): implications for fluid/rock interaction in slow spreading environments. *Chemical Geology* 234, 179–210.
- Peucker-Ehrenbrink, B., Hanghøj, K., Atwood, T., Kelemen, P.B., 2012. Rhenium–osmium isotope systematics and platinum group element concentrations in oceanic crust. *Geology* 40, 199–202.
- Polat, A., Hofmann, A.W., 2003. Alteration and geochemical patterns in the 3.7–3.8 Ga Isua greenstone belt, West Greenland. *Precambrian Research* 126, 197–218.
- Polat, A., Hofmann, A.W., Rosing, M.T., 2002. Boninite-like volcanic rocks in the 3.7–3.8 Ga Isua greenstone belt, West Greenland: geochemical evidence for intra-oceanic subduction zone processes in the early Earth. *Chemical Geology* 184, 231–254.
- Polat, A., Hofmann, A.W., Münker, C., Regelous, M., Appel, P.W.U., 2003. Contrasting geochemical patterns in the 3.7–3.8 Ga pillow basalt cores and rims, Isua greenstone belt, Southwest Greenland: implications for postmagmatic alteration processes. *Geochimica et Cosmochimica Acta* 67, 441–457.
- Polat, A., Frei, R., Appel, P.W., Fryer, B., Dilek, Y., Ordóñez-Calderón, J.C., 2008. An overview of the lithological and geochemical characteristics of the Mesoarchean (ca. 3075 Ma) Ivisartoq greenstone belt, southern West Greenland. In: Condie, K.C., Pease, V. (Eds.), *When did plate tectonics begin on planet Earth*. Geological Society of America Special Paper, 440, pp. 51–76.
- Polat, A., Appel, P.W.U., Fryer, B.J., 2011. An overview of the geochemistry of Eoarchean to Mesoarchean ultramafic to mafic volcanic rocks, SW Greenland: implication for mantle depletion and petrogenetic processes at subduction zones in the early Earth. *Gondwana Research* 20, 255–283.
- Polat, A., Fryer, B.J., Samson, I.M., Weisener, C., Appel, P.W., Frei, R., Windley, B.F., 2012. Geochemistry of ultramafic rocks and hornblende veins in the Fiskenesst layered anorthositic complex, SW Greenland: evidence for hydrous upper mantle in the Archaean. *Precambrian Research* 214, 124–153.
- Pope, E.C., Bird, D.K., Rosing, M.T., 2012. Isotope composition and volume of Earth's early oceans. *Proceedings of the National Academy of Sciences* 109, 4371–4376.
- Rizo, H., Boyet, M., Blichert-Toft, J., Rosing, M.T., 2013. Early mantle dynamics inferred from <sup>142</sup>Nd variations in Archaean rocks from southwest Greenland. *Earth and Planetary Science Letters* 377, 324–335.
- Robinson, P.T., Malpas, J., Dilek, Y., Zhou, M.-F., 2008. The significance of sheeted dike complexes in ophiolites. *GSA Today* 18, 4–10.
- Rollinson, H., 2002. The metamorphic history of the Isua Greenstone Belt, west Greenland. Geological Society, London, Special Publications 199, 329–350.
- Rollinson, H., 2003. Metamorphic history suggested by garnet–growth chronologies in the Isua Greenstone Belt, West Greenland. *Precambrian Research* 126, 181–196.
- Rollinson, H., 2007. Recognising early Archaean mantle: a reappraisal. *Contributions to Mineralogy and Petrology* 154, 241–252.
- Rollinson, H., Appel, P.W.U., Frei, R., 2002. A metamorphosed, Early Archaean chromitites from West Greenland: implications for the genesis of Archaean anorthositic chromitites. *Journal of Petrology* 43, 2143–2170.
- Rose, N.M., Rosing, M.T., Bridgwater, D., 1996. The origin of metacarbonate rocks in the Archaean Isua supracrustal belt, West Greenland. *American Journal of Science* 296, 1004–1044.
- Rosing, M.T., 1989. Metasomatic alteration of ultramafic rocks. *Fluid Movements—Element Transport and the Composition of the Deep Crust* NATO ASI Series. volume 281. Springer, Netherlands, pp. 187–202.
- Rosing, M.T., Rose, N.M., 1993. The role of ultramafic rocks in regulating the concentrations of volatile and non-volatile components during deep crustal metamorphism. *Chemical Geology* 108, 187–200.
- Rosing, M.T., Rose, N.M., Bridgwater, D., Thomsen, H.S., 1996. Earliest part of the Earth's stratigraphic record: a reappraisal of the >3.7 Ga Isua (Greenland) supracrustal sequence. *Geology* 24, 43–46.
- Säntti, J., Kontinen, A., Sorjonen-Ward, P., Johanson, B., Pakkanen, L., 2006. Metamorphism and chromite in serpentinized and carbonate–silica-altered peridotites of the Paleoproterozoic Outokumpu–Jormua Ophiolite Belt, Eastern Finland. *International Geology Review* 48, 494–546.
- Savard, D., Barnes, S.-J., Meisel, T., 2010. Comparison between Ni–fire assay Te–coprecipitation and isotope dilution with high pressure asher acid digestion for the

- determination of platinum-group elements, rhenium and gold. *Geostandards and Geoanalytical Research* 34, 281–291.
- Schoenberg, R., Kamber, B.S., Collerson, K.D., Moorbath, S., 2002. Tungsten isotope evidence from 3.8-Gyr metamorphosed sediments for early meteorite bombardment of the Earth. *Nature* 418, 403–405.
- Snow, J.E., Dick, H.J.B., 1995. Pervasive magnesium loss by marine weathering of peridotite. *Geochimica et Cosmochimica Acta* 59, 4219–4235.
- Suárez, S., Prichard, H.M., Velasco, F., Fisher, P.C., McDonald, I., 2010. Alteration of platinum-group minerals and dispersion of platinum-group elements during progressive weathering of the Aguablanca Ni–Cu deposit, SW Spain. *Mineralium Deposita* 45, 331–350.
- Szilas, K., Garde, A.A., 2013. Mesoarchaeal aluminous rocks at Storø, southern West Greenland: new age data and evidence of premetamorphic seafloor weathering of basalts. *Chemical Geology* 354, 124–138.
- Szilas, K., Næraa, T., Scherstén, A., Stendal, H., Frei, R., van Hinsberg, V.J., Kokfelt, T.F., Rosing, M.T., 2012a. Origin of Mesoarchaeal arc-related rocks with boninite/komatiite affinities from southern West Greenland. *Lithos* 144, 24–39.
- Szilas, K., Elis Hoffmann, J., Scherstén, A., Rosing, M.T., Windley, B.F., Kokfelt, T.F., Keulen, N., van Hinsberg, V.J., Næraa, T., Frei, R., Münker, C., 2012b. Complex calc-alkaline volcanism recorded in Mesoarchaeal supracrustal belts north of Frederikshåb Isblink, southern West Greenland: implications for subduction zone processes in the early Earth. *Precambrian Research* 208, 90–123.
- Szilas, K., Hoffmann, J., Scherstén, A., Kokfelt, T.F., Münker, C., 2013a. Archaean andesite petrogenesis: insights from the Grædefjord Supracrustal Belt, southern West Greenland. *Precambrian Research* 236, 1–15.
- Szilas, K., van Hinsberg, J., Kisters, A.F.M., Hoffmann, J.E., Kokfelt, T.F., Scherstén, A., Windley, B.F., Münker, C., 2013b. Remnants of arc-related Mesoarchaeal oceanic crust in the Tartoq Group, SW Greenland. *Gondwana Research* 23, 436–451.
- Szilas, K., Hoffmann, J.E., Münker, C., Dziggel, A., Rosing, M.T., 2014a. Eoarchean within-plate basalts from southwest Greenland: comment. *Geology* 42, e330–e330.
- Szilas, K., van Hinsberg, J., Creaser, R., Kisters, A.F.M., 2014b. The geochemical composition of serpentinites in the Mesoarchaeal Tartoq Group, SW Greenland: Harzburgitic cumulates or melt-modified mantle? *Lithos* 198–199, 103–116.
- Szilas, K., van Gool, J.A.M., Scherstén, A., Frei, R., 2014c. The Mesoarchaeal Storø Supracrustal Belt, Nuuk region, southern West Greenland: an arc-related basin with continent-derived sedimentation. *Precambrian Research* 247, 208–222.
- Takahashi, E., Uto, K., Schilling, J.G., 1987. Primary magma compositions and Mg/Fe ratios of their mantle residues along Mid Atlantic Ridge 29° to 73° N. Institute for Study of the Earth's Interior, Okayama University.
- Takazawa, E., Frey, F.A., Shimizu, N., Obata, M., Bodinier, J.L., 1992. Geochemical evidence for melt migration and reaction in the upper mantle. *Nature* 359, 55–58.
- Thakurta, J., Ripley, E.M., Li, C., 2008. Geochemical constraints on the origin of sulfide mineralization in the Duke Island Complex, southeastern Alaska. *Geochemistry, Geophysics, Geosystems* 9, Q07003.
- Touboul, M., Liu, J., O'Neil, J., Puchtel, I.S., Walker, R.J., 2014. New Insights into the Hadean Mantle Revealed by 182W and Highly Siderophile Element Abundances of Supracrustal Rocks from the Nuvvuagittuq Greenstone Belt, Quebec, Canada. *Chemical Geology* 383, 63–75.
- Turner, S., Rushmer, T., Reagan, M., Moyan, J.-F., 2014. Heading down early on? Start of subduction on Earth. *Geology* 42, 139–142.
- Wang, J., Hattori, K.H., Stern, C., 2008. Metasomatic origin of garnet orthopyroxenites in the sub-continental lithospheric mantle underlying Pali Aike volcanic field, southern South America. *Mineralogy and Petrology* 94, 243–258.
- Willbold, M., Elliott, T., Moorbath, S., 2011. The tungsten isotope compositions of the Earth's mantle before the terminal bombardment. *Nature* 477, 195–199.
- Windley, B.F., Garde, A.A., 2009. Arc-generated blocks with crustal sections in the North Atlantic craton of West Greenland: crustal growth in the Archean with modern analogues. *Earth Science Reviews* 93, 1–30.
- Woodland, S.J., Pearson, D.G., Thirlwall, M.F., 2002. A platinum group element and Re–Os isotope investigation of siderophile element recycling in subduction zones: comparison of Grenada, Lesser Antilles Arc, and the Izu–Bonin Arc. *Journal of Petrology* 43, 171–198.
- Xie, Z., Hattori, K., Wang, J., 2013. Origins of ultramafic rocks in the Sulu Ultrahigh-pressure Terrane, Eastern China. *Lithos* 178, 158–170.